Physics – Uspekhi **39** (1) 1 – 29 (1996)

REVIEWS OF TOPICAL PROBLEMS PACS numbers: 61.80.Ba; 42.62.Hk

Laser control of processes in solids

F Kh Mirzoev, V Ya Panchenko, L A Shelepin

Contents

Abstract. The large amount of information carried by the energy, spectral, and space – time characteristics of a laser beam makes it feasible to use laser radiation to control the processes that occuring in solids. The influence of laser radiation with a wide range of deposited energies on a variety of processes is considered: these processes include crystal growth, formation of dissipative (spatial and temporal) defect structures on the surface and in the bulk of a solid, instabilities in melts, materials fracture considered from the point of view of both selectivity and self-organisation. An analysis is made of the relationship between the nature and parameters of such structures, on the one hand, and the characteristics of laser radiation, on the other.

1. Introduction

The appearance of lasers has led to drastic changes in many technological processes. These changes are related to the unique properties of laser radiation: monochromaticity, coherence, high energy densities in pulses, small dimensions of the focusing spot, and precision of control over the intensity, duration of action, and laser beam position. In the last three decades there has been considerable progress in laser technologies. They include cutting, welding, drilling of holes, surface hardening, atomisation, thermal cleaving, photochemical processes, and isotope separation [1 – 7]. Laser systems and technological lines are used widely in machine building, textile industry, car manufacture, aircraft manufacture, watch industry, and many other fields. Laser methods are often competitive in respect of cost when compared with traditional means for the processing of materials.

Laser technologies are of growing importance also in microelectronics. They are used in such operations as coating, annealing, deposition and etching of films, doping with impurities, gettering, scribing, and epitaxy [8 – 12]. Initially these laser technologies have been based on the thermal (nonspecific) action of laser radiation, but gradually new opportunities have been found for using laser radiation selectively to influence various processes in solids, the structure of materials, and the crystal growth and damage. A laser beam does not simply carry energy, but it can exhibit a complex spatial, temporal, and spectral structure. Much information can encoded in a laser beam in such a way that its effects on various processes in a solid are efficient and selective. In this sense the effects of a laser beam are of information – energy nature and provide opportunities for process control.

The very idea of process control by lasers is not new. The feasibility of controlling chemical reactions by laser radiation

F Kh Mirzoev, V Ya Panchenko Scientific-Research Centre on Industrial Lasers, Russian Academy of Sciences,
ul. Pionerskaya 2, 142092 Troitsk, Moscow Region, Russia
Tel. (7-095) 334-09092
L A Shelepin P N Lebedev Physical Institute, Russian Academy of Sciences, Leninskiĭ Prosp. 53, 117924 Moscow, Russia
Tel. (7-095) 132-67-54. Fax (7-095) 132-24-08

Received 17 March 1995; revision received 2 August 1995
Uspekhi Fizicheskikh Nauk **166** (1) 3 – 32 (1996)
Translated by A Tybulewicz, edited by A Radzig

has been discussed since 1970 [13, 14]. In a book [14] on selection of optimal laser action conditions it is pointed out that the dynamics of physical processes in a laser field is in most cases extremely sensitive to the conditions during irradiation and this makes it possible to consider radiation parameters as control factors (see also Refs [15–17]). However, the problem of control of various processes in solids considered in this review, including an analysis of the feasibility of deliberate action on the structure of crystals and preparation of materials with desired properties, has a number of special features. These features are related to the use of selective laser excitation and activation methods, and to the possibility of self-organisation under the influence of laser radiation.

Opportunities for selective action of laser radiation are determined by the specific characteristics of the process in a solid. A solid can be regarded as a complex system of excitations, stresses, and defects. The mechanical, electric, magnetic, and optical properties of a solid depend on the structure of its crystal lattice, on elementary excitations (phonons, electrons, excitons), on the systems of defects (point: vacancies, interstitial host atoms, interstitial and substitutional impurity atoms; linear: dislocations, dislocation loops; bulk: voids, microcracks, and aggregate of defects — complexes), and on stresses in the lattice. This whole complex system is characterised by a considerable variety of the processes, each of which can have its own special features and its own characteristic times. In contrast to selective processes in gas kinetics, which are governed by the resonance of laser radiation with the frequency of a transition between two levels, the selectivity in a solid may be of more general nature. Excitation of specific degrees of freedom and of particular processes depends both on the resonance frequency and on the deposited energy, as well as on the duration, intensity, and profile of a pulse. Laser radiation is thus a fine instrument, which can be used to interact selectively with various components of a system and to alter the structure and properties of a variety of materials.

A solid irradiated with a laser can be regarded as an open system which is far from equilibrium. In view of the nonlinear nature of the processes in such a system, there is (in contrast to a gaseous medium) a multitude of unstable states. The states are governed by certain critical values of the control parameters and depend on the properties of the medium and those of the incident radiation. Self-organisation processes, resulting in the formation of dissipative structures, can occur under the action of laser radiation on a solid. If we know the mechanisms of the interaction with various subsystems, we can — in principle — control the formation of structures.

An essential element for laser control is information about the object to be controlled. One specific feature of solids distinguishing them from gases, in which case we can usually ignore spatial inhomogeneities, is the decisive role played by the properties of the spatial structures: the type of the lattice, the positions and interactions of the defects, and stresses. In contrast to modern gas kinetics [18], the spatial–structural kinetics of solids is known only to an unsatisfactory degree. However, in addition to scientific information on the processes occurring in solids, there is also information of another kind: instantaneous information on specific characteristics recorded with the aid of sensors. This information can be transmitted to a computer which controls a laser system and can be used to alter the laser radiation in such a way that the desired result is achieved.

This review represents an attempt to describe systematically the kinetic processes that occur in a solid from the point of view of potential control of these processes by laser radiation. The sequence used in presentation of the review is dictated by the value of the deposited energy, because an increase in this energy reveals what is in effect a new class of the main processes: selective laser action, self-organisation of structures at temperatures below the melting point, and controlled fracture in the presence of a liquid phase.

Many of the effects reviewed below are used in laser technology. However, the actual technological applications will be considered only by way of illustration and the main attention will be concentrated on the possibility of controlling specific processes, and on the dependences of the structural parameters on the laser radiation characteristics. The future of laser technologies lies in the information aspect of the effects of laser radiation and in implementation of laser control of the processes in a solid. The literature which deals to a greater or lesser extent with the problem of laser control is enormous and we selected primarily the reviews and monographs with large numbers of citations.

2. Selective effects

2.1 Thermal mechanism. Control of laser action

In the first stage of the development of laser technologies, the thermal effects have been used and these are not selective.

The overall scheme of processes proceeded in a solid under laser irradiation reduced to successive treatment of radiation absorption and heat transfer inward the bulk [1–4]. The energy flux $I(z)$ in a medium at a distance z from the surface can be described by the relationship

$$I(z) = I(0)\exp(-\alpha z)\,,$$

where α is the absorption coefficient. The bulk of the energy is absorbed in a layer of thickness $\delta \approx \alpha^{-1}$. For the majority of metals the thickness of this layer in the visible and infrared ranges of spectrum is $\delta < 0.1$ μm, which is on the order of the skin layer thickness. For a considerable number of organic compounds this thickness is $\delta < 1$ μm, i.e. in such cases the absorption of laser radiation occurs on the surface. The process of heat transport into the interior of a medium is described by

$$\rho C\,\frac{\partial T}{\partial t} = \varkappa \Delta T + Q\,,$$

where ρ is the density; C is the specific heat; $\varkappa$ is the thermal conductivity; Q is the density of the heat sources in a solid. Detailed calculations of the thermal conditions under specific technological conditions can be found in many reference sources [4, 6].

At radiation intensities $I \geqslant 10^5$ W cm^{-2}, an important role is played by the processes of melting, evaporation, and atomisation (in the last case the separate droplets acquire energy sufficient to overcome the surface tension forces). The thermal balance makes it possible to determine the shape and dimensions of the molten region. It has been found that additional technological operations are needed. For example, the conditions for efficient delivery of energy into a material requires removal of the resultant vapour [10]. When steels and titanium are cut, this is done by employing a jet of oxygen, or a jet of chlorine is used in the cutting of copper. Argon and

nitrogen jets prevent carbonisation of a material, cool the cut edges, and remove the resultant particles when cloth, plastics, plywood, and paper are cut.

The advantages of laser technologies over traditional methods include the absence of direct contact between an energy source and a material. In many industrial operations the use of laser technologies makes it possible to avoid the use of tools, drills, flames, electrodes, and chemicals. This reduces the production costs and ensures 'cleaner' technological operations. An example which illustrates this is the cutting of cloth in the garment industry. Mechanical cutting of cloth has been one of the most complex and labour-intensive operations. Distortions of the cut profile, resulting from vibrations of the working tool in a ribbon cutting machine, produce a poorer cut. The very first prototype systems for the cutting of cloth with the aid of a cw CO_2 laser have been able to deliver an increase in the productivity and an improvement in the cut quality. The simplicity of manipulation of a laser beam opens up opportunities for control of technological processes by means of computers, which is very convenient for short-run and unit production.

Combination of laser technologies with programmed control has proved particularly effective in microelectronics. For example, in the manufacture of integrated circuits in accordance with a given programme, it is necessary to make drawings of the masks to be used later; in laser lithography the resolution can be at submicron level [19]. The use of lasers can increase by an order of magnitude the productivity, compared with the traditional optical and electron beam systems. Laser technologies can now be used in all the operations employed in semiconductor electronics when integral circuits are made. The use of laser methods for nondestructive monitoring of the quality of electronic devices is growing. A system which can monitor the precision of assembly of electronic equipment is described in Ref. [20]. Every second the system calculates 2×10^5 three-dimensional coordinates of illuminated spots on the surface of an object.

Even the very first stages of the development of laser technologies have revealed that the effects of laser radiation are not purely thermal. Heating is accompanied by deformation, motion of defects, and generation of acoustic and shock waves [1, 6, 8]. Moreover, it has been found that the thermal mechanism is of very limited validity as the basis for analysis of the laser effects. This mechanism plays the dominant role within definite limits of the energy, spectral, spatial, and temporal characteristics of laser radiation. For example, when the pulse duration is short, we have to consider not simply the thermal effect, but the interaction of radiation with the conduction-electron and phonon subsystems. In local spatial action the resultant temperature gradients induce strains, stresses, and motion of defects. In contrast to gases for which the concept of selectivity of the laser radiation effects can be reduced to resonant excitation of atoms and molecules [21], solids have a spatial structure and one can speak of selective action on the various elements of this structure even in the case of the thermal mechanism. This is related to the feasibility of a high concentration of the laser radiation energy in small regions and the appearance of local nonequilibrium processes.

For example, thermally induced fracture is accompanied by a whole range of processes: evaporation of the bound (crystallisation) water, producing of high internal pressures resulting in the formation of microcracks, occurrence of irreversible chemical reactions and phase transformations, all of which weaken the internal bonds and reduce the strength. The local effects and the appearance of high temperature gradients ($10^9 - 10^{10}$ K cm^{-1}) create thermal stresses which make controlled splitting of materials possible.

Laser radiation in fact induces a large number of processes in a solid and the heating is just one of them. Two mutually related approaches have gradually crystallised when dealing with the tasks encountered in the development and applications of laser technologies. One of them is based on the development of equipment which can be used to control the laser action and the other is the search for ways acting selectively on the processes that occur in a solid and choosing in each case a laser 'key' in the form of radiation with specific characteristics.

2.2 Nonthermal effects

Various applications of lasers, which cannot be reduced to simple heating of materials, have been proposed in the seventies. A considerable role in the understanding of the mechanisms of the observed phenomena has been played by results of investigations of various nonthermal effects on solids and on the growth of crystal structures: these include the effects of electromagnetic radiation, electric fields, electron beam, and ultrasound. A shared feature of these effects is their selective nature. For example, the effects of electromagnetic radiation on the growth of crystal films and their properties have proved very critical in respect to the selection of the conditions during irradiation, the intensities and durations of the pulses, and their spectral composition. The observed selectivity is related to the effects on specific relaxation processes in a solid or on different stages of crystal growth.

A series of experimental investigations, initiated by the work reported in Ref. [22], has proved that irradiation can have a significant influence on epitaxial growth and on the quality of the resultant materials. Very detailed investigations have been made into the growth of PbTe, $Pb_{1-x}Sn_xTe$, and HgTe films [23 – 26] in which the source of light has been an ultrahigh-pressure xenon lamp with an output power of 10 kW emitting in the wavelength range 0.2 – 1.5 μm with 10% of the power in the ultraviolet (UV). It has been found that if the UV radiation is selected by a filter, the film growth rate increases by two orders of magnitude: from 0.1 – 0.2 μm min^{-1} in the absence of such radiation to 6 – 15 μm min^{-1} in its presence.

Irradiation influences also the quality of epitaxial films. Single-crystal layers can form in a narrow range of the UV radiation intensities from 10 to 30 W cm^{-2}; polycrystalline layers are obtained at somewhat lower or higher intensities. When the intensity exceeds 40 W cm^{-2}, polycrystalline growth changes to the formation of flakes, i.e. the result is uncontrolled fast growth of crystals near the surface around randomly appearing crystallisation centres. Moreover, the epitaxial growth temperature can be reduced from 800 °C to 500 °C in the presence of UV radiation.

The main mechanism responsible for these effects is the formation of free atoms [23]. UV radiation dissociates Te_2 ($E_{diss} = 2.8$ eV) and PbTe ($E_{diss} = 2.7$ eV) molecules which reach the growth surface. In the conventional process, i.e. in the absence of UV radiation, the molecular bonds break (which is necessary to ensure that an atom reaches its place in the lattice) on the surface. The probability of such bond breaking increases with the substrate temperature. Incorporation of one atom in the lattice requires $10^3 - 10^4$ collisions

of molecules with the surface of a growing crystal. In contrast to the reactions between molecules, those involving free atoms and radicals are of zero-barrier nature and the cross sections are on the order of the gas-kinetic values. This is the reason for the increase in the growth rate. Even a fraction of 1% of free atoms can influence significantly the epitaxial growth rate. The epitaxial growth temperature can be lowered because, in the presence of free atoms, a reduction in the substrate temperature and, consequently, in the probability of bond breaking in the molecules interacting with the surface does not play a significant role.

UV irradiation can also influence all the stages of crystal growth which usually occurs in accordance with the layer mechanism [27]: transfer of molecules from a vapour to an adsorption layer, surface diffusion of the adsorbed molecules on the surface to a step, diffusion along the edge of a step to a kink, and incorporation in the lattice. Such irradiation generates a surface charge, alters the adhesion properties [28], and gives rise to adsorption centres thus transferring surface atoms to excited metastable states with modified valence properties. This stimulates the formation of films on substrates on which ordinarily these films would not have grown [29]. Experimental observations indicate an improvement of the quality and a reduction in the number of defects (dislocations, micropores) in epitaxial films grown under the influence of UV radiation [24, 26].

There is thus a whole range of mechanisms by which electromagnetic radiation can influence epitaxy. Utilisation of these mechanisms provides opportunities for controlling the properties of grown epitaxial structures. This applies also to the control of the deviation of the composition of crystals from stoichiometry. The boundaries of a region of homogeneity in $P-T-x$ diagrams (P is the pressure, T is the temperature, and x is the relative concentration of a component) of binary crystals are set by the maximum permissible differences δ_v between the numbers of vacancies of the two components at the given values of P and T. Fig. 1 shows a typical $T-x$ diagram of PbTe [24, 26]. The maximum deviation from stoichiometry occurs in a region rich in tellurium (and, consequently, rich in lead vacancies). We can see that the number of excess vacancies $\delta_v = n_{Pb} - n_{Te}$ can reach $\sim 10^{19}$ cm^{-3}, i.e. it represents 10^{-3} of the total number of the lattice sites. The relationship [30]

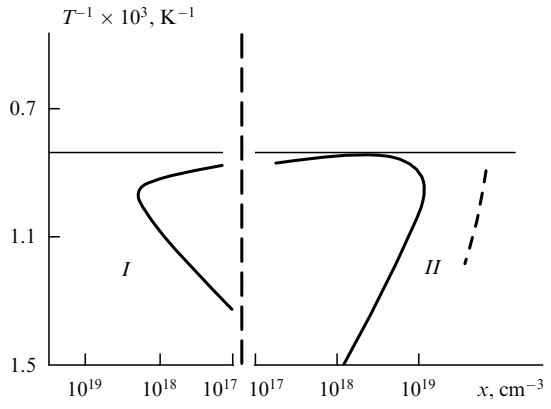

Figure 1. Homogeneity region of a PbTe crystal: (*I*) n-type; (*II*) p-type. The dashed curves are the boundaries at which a deviation from stoichiometry is observed in a defect-free crystal.

$$n_{Pb} n_{Te} = N_0 \exp\left(-\frac{E_{Te} + E_{Pb}}{kT}\right) = \mu_0$$

shows that the number of vacancies is

$$n_{Pb} = \sqrt{\frac{\delta_v^2}{4} + \mu_0} + \frac{\mu_0}{2}\,, \qquad n_{Pb} = \sqrt{\frac{\delta_v}{4} + \mu_0} - \frac{\mu_0}{2}\,.$$

Here, N_0 is the number of the lattice sites and $E_{Pb} + E_{Te}$ is the energy of formation of a pair of vacancies in the different sublattices.

When the boundary of a homogeneity region is crossed during, for example, cooling of a crystal, the excess component forms precipitates separated by distances of several tens of nanometres [31].

An increase in the degree of deviation from stoichiometry and, consequently, an increase in the number of vacancies reduces the strength of a crystal because of an increase in the number of broken bonds. This reduction in the strength makes a homogeneous structure unstable even at relatively low stresses. The boundaries of a homogeneity region are determined by a reduction in the strength of a binary crystal because of deviation from stoichiometry and by the presence of stresses associated with structure defects (pores at relatively high temperatures, cracks and dislocations at low temperatures).

Electromagnetic radiation which influences the reduction in the number of defects reduces the internal stresses, so that it is possible to go beyond the usual boundaries of a homogeneity region [25]. However, the maximum deviation from stoichiometry cannot exceed 0.1% and the presence of even weak stresses within this range makes the structure unstable. Therefore, electromagnetic radiation provides means for effective control of epitaxial growth processes, deviations from stoichiometry, and the structure of grown crystals.

The discovery of the photoplastic effect [32] played an important role in the analysis of the influence of irradiation on a system of defects and stresses in a solid. At the moment of illumination with visible light the stress flow in the crystal undergoing plastic deformation increases and this stress returns to the initial value after the end of illumination. The mechanism of this effect is a change in the conditions of the electric interaction of moving dislocations with point centres whose charge is altered by illumination and which have local levels in the band gap. Other phenomena associated with this mechanism have since been discovered: they include infrared quenching [33], the impurity photoplastic effect [34], the deformation luminescence and injection-plastic effect [35]. Moreover, it has been shown that a system of defects is related to the electric and mechanical properties of crystals and to the ability to control these properties by irradiation.

These selective effects of incoherent radiation on the processes occurring in a solid are produced also by laser radiation. However, investigations involving laser radiation have led to the discovery of a whole range of new phenomena which can be divided arbitrarily into the effects on the growth and structure of crystals and the effects on the defect subsystems.

2.3 Influence of laser radiation on the growth and structure of crystals

New opportunities for the control of vapour epitaxy are provided by the use of pulsed UV lasers. The distinguishing features of the action of UV laser pulses on crystals include a

high surface quality, an increase in the lattice constant (representing a reduction in the number of vacancies), different concentrations of defects within a laser spot and outside it (when the whole sample is illuminated simultaneously with a xenon lamp), and differences in doping under the action and in the absence of laser radiation. The growth and formation of nonplanar structures (humps) are accelerated in the laser spot [36, 37]. The results have been interpreted by considering the mechanism of the appearance of acoustic waves as a result of the thermo-optical effect. In the region where light is absorbed a change in the density creates a pressure pulse. When use is made of a UV laser with a pulse duration 10^{-8} s and of 10^4-10^5 W cm^{-2} intensity, a typical order of pressure in the investigated substances is 10^7 dyn cm^{-2} [38]. The resultant increase in the density reduces the total number of vacancies and also of various other structure defects, and is responsible for the increase in the lattice parameter. The increase in the film growth rate is evidently related to a reduction in the growth energy barrier by an amount ΩP (P is the amplitude of an acoustic wave and Ω is the activation volume) when an acoustic wave is excited.

Under real conditions we are dealing with a whole range of mechanisms which are triggered by electromagnetic radiation and have a variety of spatial, temporal, and spectral characteristics. Therefore, in a number of cases it has proved helpful to select combined regimes for the optimal control of the properties of the resultant structures. For example, an experimental investigation was made [39] of the combined influence on the epitaxial growth of PbTe and $Pb_{1-x}Sn_xTe$ of UV radiation from a cw He–Cd laser ($\lambda = 0.43$ μm, 20 mW power), a pulsed nitrogen laser ($\lambda = 0.337$ μm, pulse duration 10^{-8} s, pulsed power density 10^4-10^5 W cm^{-2}), and a xenon lamp.

Illumination with these sources increases the rate of growth of epitaxial PbTe films: when only the xenon lamp is used, the growth rate is 2.5 μm min^{-1}; under the combined influence of this lamp and the cw laser, the latter is 3.5 μm min^{-1}, and the combined effect of the lamp and the pulsed nitrogen laser increases the growth rate to 4.8 μm min^{-1}. In the regions affected by laser radiation there are humps of area similar to the size of the laser spot. The thickness and structure of these humps depend on the irradiation conditions. Under the action of the lamp and the laser the height of a hump above the film surface is 30 μm if the cw laser is used, 60 μm (and the surface of the film is mirror-smooth) when the pulsed laser is employed, and the thickness of the film which grows under the influence of the lamp alone is 60 μm.

The transverse dimension of details of the surface relief of nonplanar films is determined by the capabilities of laser focusing and the height is governed by the duration of laser irradiation. The growth of any specific structures is reproducible, suggesting that it should be possible to fabricate nonplanar objects of complex shape, to produce a given relief, and also to use nonplanar structures in different forms of data storage.

The degree of 'perfection' of epitaxial films grown in the presence of laser radiation [39] has been estimated on the basis of the density of the etch pits. The results are given in Table 1. It is evident from this table that the films grown under the influence of the lamp and the pulsed UV laser radiation have the lowest dislocation density. Investigations of the threshold temperature for epitaxial growth of PbTe show that the temperature of growth of single-crystal lead telluride films on BaF_2(111) substrates decreases from 800 °C to 300 °C under the action of the lamp and the pulsed UV laser practically without a change in the high growth rate (4.5–4.8 μm min^{-1}). The threshold temperature for the onset of growth of a single crystal is 380 °C. Under the action of the lamp and the cw UV laser the threshold temperature is 450 °C, whereas in the presence of the xenon lamp alone it is 550 °C. Moreover, the action of the pulsed laser increases also the lattice constant, which is clearly related to a reduction in the number of vacancies. There are differences also in the concentration of defects, in the quality of a crystal, in the degree of doping (resulting, in particular, in the formation of p–n junctions), and in the distribution of the charge density between the regions subjected and not subjected to the action of laser radiation.

Table 1. Dislocation density (in cm^{-3}) for epitaxial films

Epitaxial films	Xenon lamp	Xenon lamp and cw UV laser	Xenon lamp and pulsed UV laser
PbTe–BaF_2 (111)	5×10^4	2×10^4	8×10^3
PbTe–PbTe (100)	3×10^4	1×10^4	5×10^3

The selective nature of the laser radiation effects is observed also when oxide films are formed on metal surfaces. This topic has attracted attention because of attempts to increase the absorptivity of metals, which is known to fall with increase in the wavelength [4]. For example, in the case of a CO_2 laser emitting at $\lambda = 10.6$ μm the absorptivity represents only a few percent, but in the presence of oxide films it can increase to 50%–90%.

It has been shown [40–42] that the oxidation of metals in air is much faster under the influence of laser radiation than as a result of simple heating. The dual nature of this effect has been established. First, there are the photoprocesses typical of laser oxidation of semiconductors or metals, whose oxides have semiconducting properties [43]. The lower limit of these processes is set either by the band gap of the oxide or by the binding energy of the impurity levels. Second, there are the thermochemical processes induced by the high rates of change of temperature and high temperature gradients in the surface layer [41]. The transport of reagents in the solid phase and the kinetics of the oxidising reaction are influenced greatly by electric fields, and also by diffusion along grain boundaries and microcracks, and by generation of vacancies [44]. The upper limit of such selective effects is set by nonlinearities and by the appearance of instabilities.

There is a definite range of the temporal characteristics of laser radiation that is suitable for laser annealing. In microelectronics the main method for introduction of impurity atoms is implantation of high-energy (≈ 200 keV) ions. Such implantation damages the lattice of silicon, which becomes partly amorphous [8, 45, 46]. Laser annealing is carried out by means of short ($\approx 10^{-7}$ s) pulses or by scanning with a beam from a cw laser. At the end of a pulse a sample is cooled rapidly and solidifies so as to prevent a spatial redistribution of ions by diffusion. The mechanism of annealing has been interpreted in various ways: the process of heating followed by recrystallisation has been considered, as well as nonthermal formation of a dense free-carrier plasma, the electron temperature in this plasma being much higher than the lattice temperature [47].

Selective laser effects are used widely in microelectronics, particularly for chemical deposition of semiconductor, metal, and insulator films from a gas [48–51]. It is possible to form

coatings of complex configurations and micron dimensions. Laser heating of the substrate and formation of free atoms by interaction of laser radiation with a gaseous phase is used in deposition processes. Among specific technologies, it is worth mentioning the formation of silicon films [48], deposition of SiO_2 films [49], and metallisation. Photodissociation of SiH_4 and $SiCl_4$ can be induced by radiation from exciplex ArF ($\lambda = 194$ nm) and KrF ($\lambda = 248$ nm) lasers [50]. Metal-organic molecules are photodissociated when metal films are deposited.

Local heating of the substrate during laser chemical deposition of films causes pyrolysis of the compounds present in the vapour phase. Circulation of gaseous chemical compounds, which do not react with a substrate at room temperature, is set up above the substrate. Heating decomposes these compounds into components that are deposited on the substrate. As a result, the films are deposited in a local region, for example in the form of stripes or filaments with characteristic dimensions governed by the focusing of a laser beam.

2.4 Effects of laser radiation on the defect subsystem

The subsystem of defects in a solid is to some extent self-contained and it has a significant influence on the properties of a solid. Moreover, defects are very sensitive to various external stimuli. Lasers can be used to control changes in the defect subsystem. They can be used to deposit energy at a high rate in a medium: the rate of heating in the irradiation zone can reach 10^6 K s^{-1} [4]. This results in generation of point defects (vacancies and interstitial atoms). High-power laser pulses ($I = 10^7 - 10^8$ W cm^{-2}) can produce a shock wave and then defect generation occurs throughout a solid that has been crossed by the shock-wave front. At moderate intensities ($I = 10^4 - 10^7$ W cm^{-2}) when the laser spot diameter is 200–300 μm (industrial conditions) and a shock wave does not form, the main role is played by the thermal defect generation mechanism [the rate of generation is then $\mathcal{G} \propto \exp(-E_f/kT)$, where E_f is the defect formation energy and k is the Boltzmann constant] with localisation in the subsurface layer of a crystal [52].

An important role in changing the concentration of nonequilibrium point defects may be played also by extended defects (dislocations, pores, cracks), which (like the surface) can act as both sources and sinks. The concentration of point defects in a crystal exposed to laser radiation can exceed the equilibrium value by several orders of magnitude. This applies particularly to vacancies since the rapidly moving interstitial atoms quickly emerge on the surface or are absorbed by sinks inside a crystal. In the simplest case the kinetics of changes in the vacancy concentration n can be described by the equation

$$\frac{\partial n}{\partial t} + \operatorname{div} \mathbf{j} = \frac{n - n_{eq}}{\tau_0} ,$$

where τ_0 is the diffusion time of vacancies moving between sinks and sources; n_{eq} is the equilibrium concentration of vacancies; $\tau_0 = L_0^2/D$; L_0 is the average distance between the sources and sinks; $\mathbf{j}$ is the flux of defects which in the simplest case can be described by [53]

$$\mathbf{j} = -D\left(\nabla n + \frac{k_T \nabla T}{kT}\right) ,$$

where k_T is the thermal-diffusion ratio representing the transport of heat in a solid.

Laser radiation can alter, within wide limits, the concentration of nonequilibrium defects and this provides an opportunity for deliberate and selective influence on mechanical, electric, optical, and thermophysical properties of a solid. If a laser pulse is used to heat a metal to a certain temperature and the metal is then cooled rapidly in a time shorter than τ_0, some of the equilibrium defects do not manage to reach an equilibrium state and the nonequilibrium vacancies become frozen-in. There is an optimal pulse duration t_0 which maximises the number of such frozen-in vacancies [54]. This optimal duration is determined by the fact that when the pulses are short, $\tau < t_0$, a number of generated vacancies is not sufficient, but when the pulses are long ($\tau > t_0$), the rate of cooling becomes less and a most portion of the generated vacancies is not frozen-in. For example, for aluminium, iron, and several other metals the value of t_0 is $\sim 10^{-3}$ s.

Laser pulses can generate high concentrations of nonequilibrium vacancies ($n \sim 10^{17} - 10^{20}$ cm^{-3}) in surface layers of metals [55]. This alters the optical properties of metals and, in particular, it increases the absorptivity, because of the additional scattering of the conduction electrons in the skin layer by excess nonequilibrium vacancies [56]. This effect can be used in the processing of materials characterised by high reflection coefficients. For example, aluminium reflects 90%–95% of CO_2 laser radiation ($\lambda_L = 10.6$ μm). An increase in the absorptivity by the use of a pulsed laser then makes it possible to utilise efficiently the radiation from a cw CO_2 laser in the processing of metals.

The appearance of nonequilibrium vacancies reduces the service life of the reflecting coatings (mirrors) in pulsed lasers because of accelerated diffusion of the substrate atoms into the coating [40]. This effect influences also the acceleration of the growth of oxide films [55] and the mutual diffusion of components in semiconductor systems of the $Cd_{1-x}Hg_xTe$–CdTe type [57].

Laser irradiation not only alters the rates of the diffusion processes, but it can also stop these processes and even reverse their direction. For example, laser heating may cause not only evaporation, but also considerable growth of pores and dislocation loops [58].

Laser radiation can influence also the relaxation of elastic stresses and the motion of extended defects, particularly the motion of dislocations in crystals. UV laser radiation charges the surface of a crystal positively and dislocations carry a negative charge. This creates an electric field which draws dislocations to the surface [59]. The velocity of a dislocation motion v_d is directly proportional to the vacancy flux: $v_d \propto Dn$. An increase in the impurity content, when the vacancy concentration decreases, slows down the motion of dislocations and hinders their climb to the surface.

Laser radiation can be used to control the properties of transition layers which appear at heterojunctions and in stressed regions in the lattice. A typical example is a transition layer at the interface between a substrate and a film. Such a layer forms because of the mismatch between the lattice constants and because the thermal expansion coefficients are different on either side of the interface. The layer thickness is governed by the concentrations of various defects (impurities, dislocations) in the vicinity of the heterojunction.

A combined photostimulated epitaxial regime was used [39] to grow $Pb_xSn_{1-x}Te$ films. This regime involved the use of UV radiation from a pulsed nitrogen laser and of a xenon lamp. Variation of the growth temperature made it possible to

reduce the transition layer thickness from 1.5 to 0.5 μm and to lower severalfold the dislocation density. Measurements of the carrier concentration in indium-doped $Pb_xSn_{1-x}Te$ films showed that indium present in amounts of 0–0.45% has donor properties and alters the carrier concentration from 5×10^{19} to 5×10^{18} cm^{-3} ($x = 0.22$) and from 5×10^{18} to 4×10^{16} cm^{-3} ($x = 0$). When indium is present at higher concentrations (up to 0.7%, in terms of atomic fractions), it has acceptor properties and can reduce the electron concentration to 1.3×10^{14} cm^{-3}. When the indium content exceeds 0.7%, the carrier concentration increases again to 1.3×10^{15} cm^{-3}.

A common aspect of the selective laser influence on specific processes in a solid is the existence of a definite and relatively narrow range of the radiation parameters suitable for a given process. Each process (growth of single crystals, reduction or increase in the number of dislocations, growth or evaporation of pores, changes in the surface properties, etc.) has its own range. The results of going beyond these ranges and also of major changes in the irradiation conditions are illustrated strikingly in the report given in Ref. [39] describing how photostimulated epitaxy of PbTe was induced with a pulsed nitrogen laser and a xenon lamp (0.6 kW power with filters transmitting only the ultraviolet part of the spectrum). The intensity of the nitrogen laser radiation was kept constant, but the intensity of the radiation from the xenon lamp was varied by altering the current through it from 30 to 200 A. A continuous film was formed in 30 min and usually its thickness inside the laser spot was 120 μm, but outside it the desired quantity came out to 60 μm. The current through the xenon lamp was then increased and after 10 min the film was separated from the substrate (this process was reproducible in 70% of the cases). At this stage the film thickness was, respectively, 160 and 80 μm. The current comprising 125–130 A has been established para to the threshold of peeling off.

Similar results were observed also when only the xenon lamp or only the nitrogen laser was used. At a fixed radiation intensity after growth for 30 min (when the film thickness reached 60 μm) the substrate temperature increased from 650 °C to 800 °C. The rate of film growth decreased and again peeling off was observed.

It was found that the film thickness at which peeling off took place was approximately the same even when the irradiation conditions were varied in a very wide range.

The mechanism of such peeling off of films involves the motion of defects to the film–substrate interface. During the initial stage of the process when the film is still thin, the main sink for the vacancies is the surface. When a certain critical film thickness is reached, so that the escape to the surface can be ignored, the concentration of vacancies in the film begins to rise, particularly in the transition layer between the film and the substrate. When the regime is altered (by increasing the radiation intensity or increasing the temperature) the concentration of vacancies rises significantly. The resultant positive feedback between the vacancy subsystem and the field of bending strains leads to the formation of regions of high supersaturation in places of vacancy localisation (these are compressed regions), which is necessary for the appearance and growth of pores [60]. As a result, it is in these regions that adhesion of the film to the substrate becomes weaker and the film peels off.

It therefore follows that the range of such selective influence on the processes in a solid is governed by the threshold of initiation at the lower limit and by nonlinearities and the appearance of positive feedback at the upper limit.

3. A solid as an open system. Instabilities

3.1 Nonlinear processes and formation of dissipative structures

When the deposited energy is increased and the situation goes beyond the range of selective action of laser radiation, it is essential to take account of the nonlinear nature of the processes and to analyse the possibility of appearance of instabilities and the formation of ordered structures.

A solid subjected to laser radiation can be regarded as an open system and one can use the methods of synergetics in describing the instabilities and self-organisation [61, 62]. In accordance with the synergetic approach, instabilities appear at certain definite (critical) values of the parameters and the process of formation of dissipative structures is the result of competition between a large number of unstable growing modes which results in selection of the amplitude of one or several modes. The amplitudes of the dominant modes determine the type and degree of ordering, i.e. they are the order parameters.

In principle, if we know and control the parameters that represent the system and create conditions favourable for the dominance of specific modes, we can control the formation of various structures.

In analyses of the conditions for the appearance of temporal and spatial dissipative structures the studies of the dynamics of oxidation reactions on the surfaces of a material have played the role of a stimulus. A whole range of phenomena associated with instabilities and the formation of structures in a laser radiation field has been discovered. One should mention here a thermochemical instability [63–65] which appears because of positive feedback between the chemical and thermal degrees of freedom resulting from the absorptivity enhancement with increase in the oxide film thickness, the temporal dissipative structures (temperature oscillations) observed in oxidation of molybdenum [66] and several other metals [67–70], and spatial structures associated with an instability of the plane front of metal oxidation under the influence of infrared (IR) laser radiation [71–73]. The latter appear only above a certain threshold and the intensities at which they form have not only a lower but also an upper limit [72]. If a liquid oxide layer is present on the surface of a metal, an instability of the plane crystallisation front may appear [74]. In the case of vanadium pentoxide under conditions of relatively weak supercooling the usual V_2O_5 crystals are formed, but strong supercooling gives rise to dendrite crystals in the form of rectangular tubes. The free surface of V_2O_5 then increases by a factor of 10^3–10^4 (which is comparable with the increase in the surface area of powders) and can be used as a catalyst in a number of chemical and technological processes [75]. New opportunities have appeared also in the control of crystal growth and of heterochemical reactions on their surfaces [65, 68].

In the last decade the centre of attention has shifted to the studies of instabilities and self-organisation in the defect subsystem. Generation of defects may occur, in particular, as a result of pulsed laser irradiation of semiconductors under premelting conditions [76], during laser-induced oxidation [68], in the course of laser deposition of films from the gaseous phase [77], and in laser-induced etching of semiconductors

[78] and metals [79]. Defects interact with the crystal lattice and generate elastic forces. For example, a vacancy causes lattice compression with a specific reduction in the volume by $\Delta\Omega = (0.3-0.6)\Omega$ and an interstitial atom causes its expansion by $\Delta\Omega = (1.7-2.2)\Omega$ [80]. Dislocations also generate elastic strains and stresses. They are sources of an elastic field the distribution of which resembles a magnetic field created by a direct current. Similar sources of stresses are also bulk defects (pores, cracks, precipitates). In turn, all the defects experience the action of stresses in a solid and interact, via the elastic field, with one another. The defect subsystem is also coupled to phonons, conduction electrons, excitons, and other quasiparticles. For example, phonons interact directly with various defects such as vacancies, dislocations, grain boundaries, and foreign inclusions [81].

The removal of an ion in the course of formation of vacancies, introduction of an additional interstitial atom, displacement of ion cores during formation of dislocations and surface defects all give rise to uncompensated charges and create various types of charged defects that experience the action of electric forces [80].

Elastic stresses and electric forces move defects along a crystal. Many manifestations of the crystal plasticity are related directly to various types of motion of dislocations. The elastic interaction of dislocations with point defects (vacancies and impurity atoms) results in a higher concentration of these defects near dislocation axes (Cottrell clouds [80]). Impurities can block largely the motion of dislocations and stabilise them. The interaction of dislocations in their pile-ups near a dislocation wall (grain surface) may create cracks.

These nonlinear interactions may produce, under various conditions and in various materials, either periodic structures of the concentration of point defects (and also of different phases) or generate various extended defects (pores, dislocations, etc.). Surface structures appear in many forms: one- and two-dimensional lattices, concentric rings, radial and radial-ray structures, spirals, and mazes. Superlattices of point defects can appear in the bulk, for example, vacancies and N, O, or C impurity atoms form superlattices in transition metal crystals (when the concentration of these impurities ranges from 0.1 to 10 at.%) [82–85]. Superlattices of extended defects such as pores [86] or precipitates [83] can also form.

Self-organisation of structures has been observed for a great variety of temporal characteristics of radiation. For example, the observations of the effects of millisecond laser pulses include the formation of a dislocation superlattice in Si [87], whereas the effects of microsecond pulses include the formation of pores [54] and a periodic redistribution of impurities with increase in the distance from the surface [88]. Continuous laser radiation can induce concentric ring-shaped pore structures [77], nanosecond pulses can generate superlattices of point defects when the surface of Si is irradiated [89], and picosecond pulses can produce radial-ring structures when films on metal substrates are irradiated [90].

3.2 Appearance of instabilities as a result of action of laser radiation

Control of the formation of structures in a solid requires prior knowledge of the mechanisms of the relevant instabilities, development of their models, and calculations of critical conditions for the appearance of instabilities.

The instabilities that appear in a solid under the action of laser radiation can be classified in accordance with the nonlinear interactions that give rise to feedback. The early investigations have been concerned with a number of specific mechanisms: the nonlinear interaction in the course of recombination of defects at centres in the form of defect–impurity complexes [91]; the loss of stability of a homogeneous state for the subsystem of point defects associated with their upward diffusion along a concentration gradient of a substitutional impurity [92]; a mechanism due to the vacancy 'wind' effect and deviations from local neutrality on appearance of fluctuations of the impurity concentrations [93]. Although the instability mechanisms are realised under certain conditions, they are of very special nature.

Emel'yanov and his colleagues [77, 89, 94–98, 102] analysed the problem from a more general standpoint. They considered the growth of surface instabilities that can appear in a variety of situations in a system of interacting strain, temperature, and defect-concentration fields. These instabilities are known as concentration–strain–thermal (CST) [94–106]. A general idea on the development of CST instabilities has been formulated. In CST instabilities a fluctuation harmonic of the field of elastic strains in a medium modulates some parameter (band gap, defect migration energy, defect drift velocity, the rates of defect generation and recombination) which controls the spatial and temporal distributions of the defect concentration and temperature. Modulation of such parameters gives rise to periodic spatial–temporal fields of the defect concentration and temperature and, consequently, creates forces proportional to their gradients. Under certain critical conditions, these forces cause a build-up of the initial fluctuations of strains and facilitate the growth of CST instabilities characterised by an exponential increase (with time) of the amplitudes of the Fourier harmonics of the fields representing perturbations of the defect concentration and temperature. A theory of CST instabilities resulting in the formation of periodic structures has begun to develop from discussions of an electron–strain–thermal instability in the course of interband transitions in semiconductors, giving rise to a semiconductor–metal phase transition and to periodic structures of different phases [96]. In this case the role of the defect subsystem is played by electron–hole pairs. A theory of a vacancy–strain instability, associated with the appearance of strain-induced drift vacancies in free metal plates or films exposed to laser radiation and leading to various periodic vacancy–strain structures, is considered in Refs [60, 97, 100].

These instabilities appear because of an external energy flux (endothermal CST instabilities). There can be also CST instabilities growing because of internal heat evolution (exothermal CST instabilities). They include a crystallisation–strain–thermal instability in the course of laser crystallisation [102] and the recombination CST instabilities which develop because of heat evolution in the course of defect recombination [99–101, 105]. Depending on which parameter of the defect subsystem in a crystal is modulated by strains, we can distinguish three varieties of CST instabilities that have been investigated so far. In the case of the drift CST instability the activation energy of diffusion is modulated and the result is a deformation-induced drift of defects culminating in their upward diffusion [77, 85, 97, 100]. In the generation of CST instability the presence of strains alters the rates of defect generation and heat evolution [95, 98]. Finally, we have the recombination CST instability in which

strains affect the rates of recombination and disappearance of defects at sinks [101, 105].

A general model of CST instabilities is proposed in Refs [60, 100]. This model applies to a fairly large class of instabilities that appear under the action of laser radiation and some of its aspects can be applied also to instabilities of other types.

Let us consider an isotropic solid in which a concentrated energy flux (which can be a laser beam or a flux of high-energy particles) generates mobile point defects. Let $n_j(\mathbf{r}, t)$ be the concentration of defects of type j ($j = v$ for vacancies, $j = i$ for interstitial atoms, and $j = p$ for impurities) at a point $\mathbf{r}$ at a moment t: $\mathbf{r} = (x, y, z)$. The main processes that control the evolution in time of the defect subsystem are the diffusion, drift, mutual annihilation, and finally absorption at sinks. The equations describing the defect kinetics and taking account of these processes can be written in the form

$$\frac{\partial n_j(\mathbf{r}, t)}{\partial t} + \operatorname{div} \mathbf{j}_j(\mathbf{r}, t) = \mathcal{G}_j(\mathbf{r}, t) - L_j(\mathbf{r}, t)\,, \tag{3.1}$$

$$\mathbf{j}_j(\mathbf{r}, t) = -D_j \nabla n_j(\mathbf{r}, t) + \mathbf{v}_j n_j(\mathbf{r}, t)\,, \tag{3.2}$$

where $\mathcal{G}_j = \mathcal{G}_j(T, \varepsilon)$ (T is the temperature of the medium, $\varepsilon = \operatorname{div} \mathbf{u}$ is the elastic strain in the medium, $\mathbf{u}$ is the displacement vector) is the rate of generation of defects (in the case of impurities, we have $\mathcal{G}_p \equiv 0$). Eqn (3.2) represents the defect flux $\mathbf{j}_j(\mathbf{r}, t)$ and the first term in this equation corresponds to diffusion with the coefficient $D_j = D_{j0} \exp(-E_{mj}/kT)$, where E_{mj} is the activation energy of diffusion. The second term describes the drift of defects at the velocity $\mathbf{v}_j = (D_j/kT)\mathbf{F}_j$ under the influence of the force $\mathbf{F}_j = -\nabla U$ resulting from the interaction of defects with an inhomogeneous strain field (U is the energy of the interaction between one defect and the strain field: $U = -K\Omega_j \operatorname{div} \mathbf{u}$), K is the bulk modulus, Ω_j is a dilatation parameter representing the change in the volume of a crystal as a result of formation of one defect: for vacancies and small-radius impurities we have $\Omega_j < 0$, for interstitial atoms and large-radius impurities we have $\Omega_j > 0$ ($\Omega_j \approx d_0^3$, where d_0 is the lattice period). In Eqn (3.1), the last term describes defect losses as a result of mutual recombination and absorption at sinks: $L_j = L(\varepsilon, T)$.

The defects present in a crystal deform it. The resultant strains can be found from the equation of equilibrium of an elastic isotropic body [82]

$$\rho \frac{\partial^2 u_i}{\partial t^2} = \frac{\partial \sigma_{ik}}{\partial x_k}\,, \tag{3.3}$$

where u_i are the components of the displacement vector. The relationship between the components u_i and the strain tensor is $u_{ik} = (\nabla_i u_k + \nabla_k u_i)/2$ [107].

The mechanical stress tensor σ_{ik} can be deduced from the expression for the density of the free energy of an elastic continuum [81]:

$$F = K \frac{u_{ll}^2}{2} + \mu \left(u_{ik} - \delta_{ik} \frac{u_{ll}}{2} \right)^2 + \sum_j K\Omega_j u_{ll} n_j - K\alpha_T T u_{ll}\,, \tag{3.4}$$

where μ is the shear modulus and α_T is the thermal expansion coefficient. Expression (3.4) is derived on the assumption that dilatation centres are isotropic, i.e. $\Omega_{kl} = \Omega_j \delta_{kl}$. It then follows from formula $\sigma_{ik} = \partial F/\partial x_k$ that σ_{ik} can be described by

$$\sigma_{ik} = K u_{ll} \delta_{ik} + 2\mu \left(u_{ik} - \delta_{ik} \frac{u_{ll}}{2} \right) + \sum_j K\Omega_j n_j - K\alpha_T T\,.$$

Substitution of the expression for σ_{ik} into Eqn (3.3) gives the following equation for the displacement vector $\mathbf{u}$:

$$\frac{\partial^2 \mathbf{u}}{\partial t^2} = c_\tau^2 \Delta \mathbf{u} + (c_l^2 - c_\tau^2) \operatorname{grad}(\operatorname{div} \mathbf{u}) + \sum_j \frac{K}{\rho} \Omega_j \operatorname{grad} n_j - \frac{K\alpha_T}{\rho} \operatorname{grad} T + G_N(\mathbf{u})\,, \tag{3.5}$$

where c_l and c_τ are the longitudinal and transverse components of the velocity of sound [107]. The third term on the right of Eqn (3.5) describes the concentration stresses generated by defects and the fourth term represents the thermoelastic stresses associated with an inhomogeneous temperature field. The function $G_N(\mathbf{u})$ takes account of the anharmonicity of the elastic medium.

The equation for the temperature of such a medium can be written in the form

$$\rho C \frac{\partial T}{\partial t} - \varkappa \Delta T = Q + \sum_{j=i,v} \Theta_j \beta_j n_j + \Theta_{iv} \mu_R n_v n_i\,. \tag{3.6}$$

The first term on the right of Eqn (3.6), $Q = Q(T, n_j, \varepsilon)$, describes heating of the medium by an external energy flux and the other two terms represent heating by heat evolution resulting from the absorption at sinks (β_j is the absorption rate) and from mutual recombination of point defects (μ_R is the recombination probability); Θ_i, Θ_v, Θ_{iv} are the energies released per unit volume. The order of magnitude of these energies is $\Theta_j \approx E_{fj}$ (E_{fj} is the energy of formation of a defect of type j) and these energies are related: $\Theta_v + \Theta_i < \Theta_{iv}$.

In discussing the CST instability on the surface of a crystal we have to supplement Eqns (3.1)–(3.6) with the appropriate initial and boundary conditions. On a free surface ($z = 0$), we have

$$D_j \frac{\partial n_j}{\partial z} - K\Omega_j n_j \frac{D_j}{kT} \frac{\partial^2 u_z}{\partial z^2} = S_j n_j\,, \qquad \varkappa \frac{\partial T}{\partial z} = \sum_{j=v,i} \Omega_j n_j S_j\,,$$

$$\frac{\partial u_x}{\partial z} + \frac{\partial u_z}{\partial x} = 0\,, \qquad \frac{\partial u_z}{\partial y} + \frac{\partial u_y}{\partial z} = 0\,, \tag{3.7}$$

$$-\frac{K\alpha_T}{\rho c_l^2} T + \frac{K}{\rho c_l^2} \sum_{j=v,i,p} \Omega_j n_j + \frac{\partial u_z}{\partial z} + (1 - 2\beta_c) \left(\frac{\partial u_x}{\partial x} + \frac{\partial u_y}{\partial y} \right) = 0\,,$$

and for $z = \infty$, we obtain

$$n_j(x, y, \infty, t) = T(x, y, \infty, t) = n_j(\mathbf{r}, 0) = T(\mathbf{r}, 0) = 0\,, \tag{3.8}$$

where S_j is the rate of surface recombination of defects; the z axis is directed into the medium; $\beta_c = c_\tau^2/c_l^2$.

Eqns (3.1)–(3.6), in combination with the conditions represented by expressions (3.7) and (3.8), form a closed system of equations which describes uniquely the evolution of CST instabilities both on the surface and in the interior of a solid which is exposed to external energy fluxes.

Specific analyses of various instabilities will be made in the following sections. This will include derivation of the dispersion equation on the basis of a linear analysis of the stability of a stationary state of the initial system represented by Eqns (3.1) – (3.8) and also determination of the amplitudes of the appeared structures which depend on the characteristics of the incident laser radiation and on the parameters of the medium.

4. Ordered point-defect structures

4.1 Diffusion – deformation instability

Spatial structures formed from point defects generated by laser radiation of intensities in the range $10^3 - 10^5$ W cm^{-2} are observed both on the surface (or in thin films) and in the bulk of solids. Control of the formation of various structures can be based on the information carried by a laser beam. It is possible to control also the parameters and even the nature of structures formed not only as a result of various instabilities, but also within the framework of one instability. We shall consider these possibilities on the basis of a diffusion–deformation (DD) instability the physical mechanism of which can be described as follows [85, 94]. A fluctuation harmonic of an elastic strain of a medium gives rise to a deformation-induced drift of point defects. A redistribution of defects generates forces proportional to the gradient of the defect concentration ($F \propto \nabla n$). When a certain critical defect concentration n_* is exceeded, these forces amplify a small 'seed' strain leading to an instability.

We shall consider the processes leading to the DD instability in a metal film (of thickness h) on an insulator substrate, heated by focused cw laser radiation. It is assumed that the substrate is optically opaque and that the temperature field $T = T(\mathbf{r})$ is steady. The z axis is perpendicular to the film surface which lies between the $z = h/2$ and $z = -h/2$ planes. Since the film is attached only weakly to the substrate, it may experience bending leading to a drift flux of defects (vacancies). The system of equations describing the DD instability in films includes an equation for the vacancy density on the surface $n_v(z = h/2, \mathbf{r}, t) \equiv n(\mathbf{r}, t)$ and an equation for the coordinate of the flexural (bending) strain in the film $\xi(x, y, t)$, which is equal to the displacement along the z axis of the points in the medium lying on the neutral ($z = 0$) plane [60, 100]:

$$\frac{\partial n}{\partial t} = D\Delta n - \frac{DK\Omega h}{4kT}\,\mathrm{div}\left[n\,\mathrm{grad}(\Delta\xi)\right], \tag{4.1}$$

$$\frac{\partial^2 \xi}{\partial t^2} = -\frac{c^2 h^2}{12}\,\Delta^2\xi + c_\parallel^2\Delta\xi + G_N(\xi) + \frac{\sigma_\perp - \Omega K n}{\rho h}. \tag{4.2}$$

Here, $\Delta = \partial^2/\partial x^2 + \partial^2/\partial y^2$; $\Omega \equiv \Omega_v$; $c_\parallel^2 = E/(1-\sigma^2)\rho$ [107]; E is the Young modulus; σ is the Poisson ratio; $c_\parallel^2 = \sigma_\parallel/\rho$; $\sigma_\parallel$ and $\sigma_\perp$ are the axially symmetric stresses directed, respectively, along and perpendicular to the film surface and generated by spatially inhomogeneous axially symmetric heating ($\sigma_\parallel = \sigma_\perp$). The last term in Eqn (4.2) takes account of the local reduction in $\sigma_\perp$ as a result of appearance of vacancies. Eqn (4.1) is derived bearing in mind that the tensile and compressive strains are related to the film bending by $\mathrm{div}\left[\mathbf{u}(z = h/2)\right] = -(h/4)\Delta\xi$ [107] and also that $n(z = h/2) \gg n(z = -h/2)$.

A linear analysis of the stability of a spatially homogeneous solution (n_0, ξ_0) of the system of equations (4.1)–(4.2) in the presence of small inhomogeneous perturbations $n_1(\mathbf{r}, t)$ and $\xi_1(\mathbf{r}, t)$ ($n_1 \ll n_0$, $\xi_1 \ll \xi_0$) of the type n_1, $\xi_1 \propto \exp(\gamma t) J_0(\kappa \mathbf{r})$ (J_0 is the Bessel function of the zeroth order and κ is the wave number of perturbations) leads to the following dispersion equation [60]:

$$\gamma(\kappa) = D\kappa^2\left[g_\parallel(l_\parallel^2\kappa^2 + 1)^{-1} - 1\right], \qquad g_\parallel = \frac{n_0(K\Omega)^2}{4kT\sigma_\parallel}, \quad l_\parallel^2 = \frac{(hc)^2}{12c_\parallel^2}. \tag{4.3}$$

It therefore follows that if $n > n_* = 4kT\sigma_\perp/(K\Omega)^2$ there is range of wave numbers $0 < \kappa^2 < \kappa_0^2$ in which $\gamma > 0$, i.e. the amplitudes of the Fourier harmonics of the perturbations increase with time without limit. This gives rise to an instability and its growth results in the formation of coupled periodic structures of vacancies and flexural strains in the form of concentric rings.

The maximum value of the instability increment γ_m is reached for $\kappa^2 = \kappa_m^2 = (\sqrt{g_\parallel} - 1)/l_\parallel^2$:

$$\gamma_m = \frac{D(g_\parallel + 1 - 2\sqrt{g_\parallel})}{l_\parallel^2}, \tag{4.4}$$

and the period of the ring structure is

$$d = \frac{2\pi}{\kappa_m} = \frac{2\pi l_\parallel}{(\sqrt{g_\parallel} - 1)^{1/2}}. \tag{4.5}$$

These periodic ring structures of vacancies and strains are due to the appearance of a vacancy drift flux resulting from bending ($g_\parallel \neq 0$) and from the fact that $\sigma_\parallel \neq 0$ in a film ($\kappa_m \to 0$ for $\sigma_\parallel \to 0$), so that the dependence $\gamma(\kappa)$ has a maximum. Inhomogeneous fluctuations n_1 with the wave number κ_m and growing at a rate proportional to γ_m, which is several orders of magnitude the rate of growth of homogeneous fluctuations, appear against the homogeneous fluctuation background ($\kappa \equiv 0$).

The anharmonicity of the elastic continuum stabilises the resultant instability. Under steady-state conditions in the one-dimensional case (when the x axis is selected) it follows from the expression for $G_N(\xi)$ [107] that the system of equations (4.1) – (4.2) becomes

$$\frac{\partial^2 n_1}{\partial x^2} = \frac{K\Omega h n_0}{4kT}\,\frac{\partial^4 \xi_1}{\partial x^4}, \tag{4.6}$$

$$\frac{c^2 h^2}{12}\,\frac{\partial^4 \xi_1}{\partial x^4} - \frac{c^2}{2}\,\frac{\partial^2 \xi_1}{\partial x^2}\left(\frac{\partial \xi_1}{\partial x}\right)^2 - c_\parallel^2\,\frac{\partial^2 \xi_1}{\partial x^2} + \frac{\sigma_\perp \Omega}{\rho h}\,n_1 = 0. \tag{4.7}$$

Substitution in Eqns (4.6) and (4.7)

$$n_1 = n_{\kappa_m}\cos(\kappa_m x), \qquad \xi_1 = \xi_{\kappa_m}\cos(\kappa_m x) \tag{4.8}$$

gives expressions for steady Fourier amplitudes of the vacancy-concentration and flexural strain fields characterised by $\kappa = \kappa_m$ for a one-dimensional lattice, viz.

$$n_{\kappa_m} = \frac{\sqrt{6}\,c_\parallel^2}{\Omega c^2}\,g_\parallel^{5/4}(\sqrt{g_\parallel} - 1), \qquad \xi_{\kappa_m} = \frac{h g_\parallel^{1/4}}{\sqrt{6}}. \tag{4.9}$$

If a medium is isotropic and the temperature distribution $T(\mathbf{r})$ is axially symmetric, all the directions of the vector κ_m are equivalent. The resultant fields of n_1 and ξ_1 are obtained if the set of expressions (4.8) is modified by replacing $\cos(\kappa_m x)$

with $\cos(\kappa_m \mathbf{r}) = \cos(\kappa_m r \cos\varphi)$ (r and φ are the polar coordinates in the film plane) and integrating with respect to φ in the interval $(0, 2\pi)$:

$$n_1 = n_{\kappa_m} J_0(\kappa_m r)\,, \qquad \xi_1 = \xi_{\kappa_m} J_0(\kappa_m r)\,. \tag{4.10}$$

The set of expressions (4.10) describes periodic distributions of vacancies and flexural strains in a film which are in the form of concentric rings whose period is given by expression (4.5). Evolution of the DD instability in systems with two types of defects (vacancies and interstices) is considered in Ref. [100].

In addition to one-dimensional and ring lattices, the development of the DD instability in a film can also create structures in the form of radial rays. They form when the laser field has the axial symmetry and the laser radiation intensity depends strongly on the radial coordinate [96].

For example, let us assume that the intensity in a laser spot has the Gaussian distribution: $I = I_0 \exp(-r^2/r_0^2)$. Then, on the film surface ($z = h/2$), on condition that $h \ll r_0$, the temperature distribution is $T = T_0 \exp(-r^2/r_0^2)$, where T_0 is the temperature at the centre of the laser spot ($r = 0$). If we assume that the defects are generated by the thermal mechanism, their steady distribution (when $kT_0 \ll E_f$) is $n_0(r) = n_0 \exp(-r^2/r_{eff}^2)$, where $r_{eff} = r_0\sqrt{kT_0/E_f} \ll r_0$.

The equation for n_1 becomes

$$\frac{\partial n_1}{\partial t} = D\Delta n_1 - \frac{DK\Omega h n_0}{4kT}\,\Delta^2\xi \exp\left(-\frac{r^2}{r_{eff}^2}\right), \tag{4.11}$$

and the equation for ξ_1 remains unchanged.

The solution of Eqns (4.11) and (4.2) will be sought in the form of radial rays:

$$n_1, \xi_1 \propto \left(\frac{r}{r_{eff}}\right)^m \cos(m\varphi) \exp\left(-\frac{r^2}{r_{eff}^2}\right), \tag{4.12}$$

where $m \gg 1$ is an integer. Substitution of the solution, described by expression (4.12), into Eqns (4.2) and (4.11) gives the dispersion equation which is of the same form as for one-dimensional lattices provided κ^2 is replaced with $\tilde{\kappa}^2 = 4m/r_{eff}^2$. The number of rays in a structure is $m \approx \pi^2 r_{eff}^2/d^2$, where d is the lattice period. This number is found in the same way as in the preceding case, from the condition $\kappa_m^2 = \tilde{\kappa}^2$. For typical parameters $r_{eff} = 0.01$ cm and $d = 3 \times 10^{-3}$ cm, we find that $m = 10^2$.

Therefore, within the framework of a specific (DD) instability we can expect structures of different type depending on the parameters of the incident radiation and of the sample itself. Formation of one-dimensional lattices, concentric ring structures, and radial structures is determined by the spatial characteristics of the laser radiation (uniform irradiation of the whole sample, a laser spot with a uniform intensity distribution, and a circular spot with a radial dependence of the intensity). More complex structures can also form. Changes in the spatial characteristics of a laser beam provide an effective means for the control of the formation of specific (given) surface structures.

The DD instability can also be used to act on heterogeneous interfaces in a solid, particularly on film – substrate interfaces. Concentric-ring peeling off of a film was observed [77] during laser deposition of polycrystalline molybdenum films from the gaseous phase. This was associated with the development of the DD instability when fluctuations create an inhomogeneous field of flexural stresses inducing drift fluxes directed opposite to diffusion in the vacancy subsystem. Regions of compression attract vacancies and regions in tension repel them. Vacancies become localised in compressed regions and they themselves deform the film enhancing the initial fluctuations of the flexural strain. The resultant positive feedback leads to an instability and, as a consequence, to the appearance (in the regions of vacancy localisation) of a strong supersaturation sufficient for the formation and growth of vacancy clusters, viz. pores. The adhesion of a film to its substrate becomes weaker at the positions of such pore clusters and periodic concentric peeling off of the film is observed.

We shall now obtain some numerical estimates. Typical values of the constants $\Omega = 10^{-23}$ cm^3, $K = 5 \times 10^{11}$ erg cm^{-3}, $\alpha_T = 10^{-3}$ K^{-1}, $T = 500\,^\circ$C give an estimate of the critical vacancy concentration: $n_* = 8 \times 10^{18}$ cm^{-3}. Under the experimental conditions reported in Ref. [77] we have $h = 5 \times 10^{-6}$ cm, $E = 10^{11}$ erg cm^{-3}, $\sigma_\parallel = 10^9$ erg cm^{-3}, and $\sigma \ll 1$, which means that $l_\parallel \approx \sqrt{10}\,h \approx 10^{-5}$ cm. We can then substitute $g_\parallel = 1 + \delta$ (where $\delta \ll 1$) in the set of expressions (4.3). Therefore, $\delta \approx 2\kappa_m^2 l_\parallel^2 = 8\pi^2 l_\parallel^2/d_{expt}^2 \approx 10^{-2}$ if $d_{expt} \approx 3 \times 10^{-3}$ cm [77]. It follows from expression (4.4) that $\gamma_m \approx D\delta^2/2l_\parallel^2 \approx 0.5$ s^{-1} for $D \approx 10^{-6}$ cm^2 s^{-1}. Formation of a vacancy structure with a period d_{expt} occurs in a time interval $\gamma_m^{-1} \approx 2$ s, which is in full agreement with the experimental conditions [77] under which the deposition time was 20 s. Assuming that in thin films the main vacancy sink is the surface, it follows that under steady-state conditions we have $n_0 = c_1 h^2$ ($c_1 = \text{const}$). Expressions (4.3) and (4.5) then yield the period $d = 2\pi l_\parallel/(c_1 h - 1)^{1/2}$.

It follows that the formation of ring vacancy structures occurs only when the film thickness is $h > h_*$, in agreement with experiments [77].

If a film contains substitutional impurities of two types differing is respect to the diffusion activation energies satisfying the inequality $E_1 < E_a < E_2$ (E_a is the energy of migration of the host lattice atoms), it follows that as a result of diffusion the more mobile impurity atoms will collect in compressed regions and the less mobile atoms in the regions which are in tension. As a result, laser irradiation will remove impurities from the centre of a film. The characteristic time of such laser 'purification' is a fraction of a second [100].

4.2 Recombination – deformation instability

Formation of ordered defect structures in crystals containing different sinks present in high concentrations is associated with a recombination – deformation (RD) instability [99, 100] the physical origin of which is as follows. When a medium is deformed by the generation of defects, the activation barrier E of the process of defect self-diffusion near the sinks is modulated ($\tilde{E} = E + \Theta \operatorname{div} \mathbf{u}$, $E = E_f + E_m$, where Θ is the deformation potential). The associated modulation of the sink intensities (I_s) in turn leads to additional growth of the strain fluctuations and when the defect concentration exceeds a critical value, the RD instability appears as a result of positive feedback.

We shall consider first the RD instability in thin metal plates (or films) [105]. It is assumed that external pumping at a time-independent rate creates point defects in a medium (specifically, vacancies) and their concentration decreases away from the surface ($z = h/2$) with depth in the medium, and the surface diffusion and recombination coefficients exceed considerably the corresponding coefficients for the

bulk ($D_s \gg D$, $\beta_s \gg \beta$). A plate is located between the planes $z = -h/2$ and $z = h/2$. Then the kinetics of the RD instability can be described by the following system of equations [105]:

$$\frac{\partial n_s}{\partial t} = D_s \Delta n_s + \mathcal{G}_s - \sum_j I_s^j(\xi)\rho_j\,, \tag{4.13}$$

$$\frac{\partial^2 \xi}{\partial t^2} = -\frac{c^2 h^2}{12}\,\Delta^2 \xi + G_N(\xi) + \frac{\Omega K n_s}{\rho h}\,, \tag{4.14}$$

where $n_s = n(z = h/2)$ is the vacancy density on the surface of the plate [$n(z = h/2) \gg n(z = -h/2)$]; $\Delta = \partial^2/\partial x^2 + \partial^2/\partial y^2$; $\mathcal{G}_s$ is a surface source; ρ_j and I_s^j are, respectively, the density and intensity of sinks of type j. The summation in Eqn (4.13) is carried out over all the sinks: it applies to those present in the plate and those generated in the course of irradiation. When the role of sinks is played by microscopic pores (vacancy clusters) and dislocations, $I_s^j(\xi)$ is described by [116]

$$I_s^j(\xi) = Z_j\left[D_s n_s - D_0 N_0 \exp\left(-\frac{\tilde{E}(\xi)}{kT}\right)\right],$$

where N_0 is the number of lattice points; Z_j represents the efficiency of absorption of point defects by sinks of type j. For pores we have $Z_p = 4\pi R$; R is the average radius of the pores; for dislocations we have $Z_d = 2\pi/\ln(2R_d/L_d)$, $L_d = \mu b(1+\sigma)\Omega/\left[3(1-\sigma)\pi kT\right]$; R_d is the average distance between dislocations in a crystal, related to the dislocation density ρ_d by $R_d \approx (\pi\rho_d)^{-1/2}$. The parameter Z_j can vary with time. However, if the instability growth time (γ^{-1}) is considerably shorter than the characteristic time for a change in Z_j, we can assume that $Z_j = \text{const}$.

The assumption that $n_s = n_0 + n_1$, $\xi = \xi_0 + \xi_1$ and linearisation in terms of small corrections of the type $n_1 = n_\kappa \exp(\gamma t + i\kappa x) + \text{C.C.}$ and $\xi_1 = \xi_\kappa \exp(\gamma t + i\kappa x) + \text{C.C.}$, where n_κ and ξ_κ are the amplitudes of the Fourier harmonics, yields the dispersion equation for the RD instability [105]:

$$\gamma(\kappa) = -D\kappa^2 - \beta_{s0}\left(1 - 6n_0 K\Omega\,\frac{\Theta}{\rho c^2 h^2 kT\kappa^2}\right). \tag{4.15}$$

Here, $\beta_{s0} = q_s^2 D$, $q_s^2 = \sum_j Z_j \rho_j$ is the sum of the sink intensities, where q_s^{-1} is the diffusion path of a defect before it becomes absorbed by the nearest sink.

If follows from expression (4.15) that if

$$n_0 \geqslant n_*(\kappa) = (\kappa^2 + q_s^2)\,\frac{\rho(ch\kappa)^2 kT}{6K\Omega\Theta q_s^2}\,, \tag{4.16}$$

the increment $\gamma \geqslant 0$ and the RD instability develops in the plate giving rise to various structures.

Stabilisation of the RD instability can be traced to a nonlinearity of flexural strain, i.e. it occurs because of $G_N(\xi)$. When the pump parameter exceeds the critical value given by expression (4.16), steady Fourier amplitudes n_κ and ξ_κ appear and their values follow from Eqns (4.13) and (4.14) if it is assumed there that $\partial n_s/\partial t \equiv 0$:

$$\xi_\kappa = -\frac{h}{\sqrt{6}}\left(\frac{\kappa_0^2}{\kappa^2} - 1\right)^{1/2}, \qquad n_\kappa = \frac{(\kappa h)^2 n_0 \Theta}{\sqrt{24}\,kT}\left(\frac{\kappa_0^2}{\kappa^2} - 1\right)^{1/2}, \tag{4.17}$$

where $\kappa_0^2 = 6n_0 K\Theta\Omega/\left[kT\rho(ch)^2\right]$ is the maximum value of the wave vector κ; when this value is exceeded the amplitudes of the Fourier harmonics decay, because they are then characterised by $\gamma < 0$ [see expression (4.15)].

The resultant behaviour of ξ_1 and n_1 is governed by the sum of independent Fourier harmonics with the wave vectors lying in the interval $0 < \kappa < \kappa_0$:

$$n_1 = \sum_\kappa n_\kappa \exp(\gamma t + i\kappa x) + \text{C.C.}\,,$$

$$\xi_1 = \sum_\kappa \xi_\kappa \exp(\gamma t + i\kappa x) + \text{C.C.} \tag{4.18}$$

Substitution from the set of expressions (4.17) into another set (4.18) and a changeover from summation to integration, for an isotropic medium and a homogeneous distribution of the radiation intensity in a laser spot, give

$$\xi_1 = h^2\,\frac{J_1(\kappa_0 x)}{\sqrt{6}\,x}\,,$$

$$n_1 = \frac{n_0 h^3 \Theta}{4kT}\left[\frac{\kappa_0^2}{x}\,J_{-1}(\kappa_0 x) - \frac{\kappa_0}{x^2}\,J_0(\kappa_0 x) + \left(\frac{4}{\kappa_0^2 x^2} - \frac{3}{2}\right)\frac{\kappa_0^2}{x}\,J_1(\kappa_0 x) + \frac{2\kappa_0}{x^2}\,J_2(\kappa_0 x) + \frac{\kappa_0^2}{2x}\,J_3(\kappa_0 x)\right],$$

where J_ν ($\nu = -1, 0, 1, 2, 3$) are Bessel functions of the first kind.

It therefore follows that the development of the RD instability in a plate creates a lattice of coupled fields of the flexural strain and the vacancy concentration in the form of concentric rings. The period of this lattice is

$$d = 2\pi hc\sqrt{\frac{\rho kT\beta_{s0}}{6\mathcal{G}_s\Theta K\Omega}} \tag{4.19}$$

and this period grows with increase in the thickness, but decreases on increase in the defect generation rate. The formation of vacancy–strain structures as a result of the RD instability has a threshold; the increment γ governing the formation of these structures is proportional to $\mathcal{G}_s$. Since $n_0 \propto \exp(-E_f/kT)$, it follows from expression (4.19) that $d \propto T^{1/2}\exp(-E_f/2kT)$, i.e. the lattice period decreases rapidly with increase in temperature.

For typical values of the parameters of medium the RD instability threshold is $n_* = 2 \times 10^{19}$ cm^{-3}. For $n_0 = 1.1 n_*$ it follows from expression (4.19) that the period is $d = 6 \times 10^{-4}$ cm. The characteristic time of formation of surface structures as a result of the RD instability is $t_m = \gamma_m^{-1} = (n_*/n_0)\beta_{s0}^{-1} \approx 10^{-3}$ s for $\rho_d = 10^8$ cm^{-2} and $D_s = 10^{-6}$ cm^2 s^{-1}. It therefore follows that structures can appear as a result of the RD instability if the duration of the laser pulses $\tau_p \geqslant 10^{-3}$ s.

Let us now turn to the RD instability in a semi-infinite medium. Let us consider a solid which occupies the half-space $z > 0$. It is anticipated that a laser pulse is incident normally on the surface of the solid ($z = 0$) and that the distribution of the laser radiation intensity is $I = I_0 \exp(-\alpha z)$, where $I_0 = I_0(\mathbf{r})H(t)$; $H(t) = 1$ if $0 < t < \tau_p$; $H(t) = 0$ if $t < 0$ and $t > \tau_p$; $\mathbf{r} = (x, y)$. For $I_0(\mathbf{r}) = \text{const}$ and a steady temperature distribution, we have $T = T_0 \exp(-\alpha z)$. If we assume that vacancy generation is due to the thermal mechanism, then a steady homogeneous distribution of vacancies characterised by $E_f \gg kT_0$ is $n_0(z) = n_0 \exp(-\alpha_0 z)$, where $\alpha_0 = \alpha(E_f/kT_0)$. It is assumed that α_0^{-1} is much less than a typical depth of a change in $\operatorname{div} \mathbf{u}_1$.

The system of equations for fluctuations of the defect concentration n_1 and of the displacement vector of the medium $\mathbf{u}_1$ can then be written in the form

$$\frac{\partial n_1}{\partial t} = D\Delta n_1 - \beta_0 n_1 - \frac{\Theta\beta_0 n_0}{kT}\exp(-\alpha_0 z)\,\mathrm{div}\,\mathbf{u}_1(z=0), \quad (4.20)$$

$$\frac{\partial^2 \mathbf{u}_1}{\partial t^2} = c_\tau^2\Delta\mathbf{u}_1 + (c_1^2 - c_\tau^2)\,\mathrm{grad}(\mathrm{div}\,\mathbf{u}_1) - \frac{K\Omega}{\rho}\,\mathrm{grad}\,n_1\,, \quad (4.21)$$

subject to the boundary conditions

$$\begin{aligned} &\frac{\partial n_1}{\partial z}(z=0) = 0\,, \qquad n_1(z=\infty) = 0\,,\\ &\frac{\partial u_{1x}}{\partial z} + \frac{\partial u_{1z}}{\partial x} = 0\,,\\ &\frac{n_1 K\Omega}{\rho c_1^2} + \frac{\partial u_{1z}}{\partial z} + (1-2\beta_0)\frac{\partial u_{1x}}{\partial x} = 0\,. \end{aligned} \quad (4.22)$$

If on the surface ($z = 0$) the strain $\mathrm{div}\,\mathbf{u}_1 = \varepsilon_1$ is distributed in the form of one-dimensional lattices $\mathrm{div}\,\mathbf{u}_1 = A_\kappa \exp(\mathrm{i}\kappa x + \gamma t) + \mathrm{C.C.}$, the solution to Eqn (4.20) is

$$n_1 = A_\kappa \frac{q_s^2 n_0 K\Omega}{kT_0\alpha_0\delta_0}\exp(-\delta_0 z + \mathrm{i}\kappa x + \gamma t)\,, \quad (4.23)$$

where $\delta_0^2 = \kappa^2 + (\gamma+\beta_0)/D$, δ_0^{-1} is the depth of penetration of n_1 into the medium. The solution given by expression (4.23) is obtained on the assumption that $\alpha_0 \gg \delta_0$.

If the displacement vector is represented in the form $\mathbf{u} = \mathbf{u}_l + \mathbf{u}_\tau$ ($\mathrm{div}\,\mathbf{u}_\tau = 0$, $\mathrm{curl}\,\mathbf{u}_l = 0$) [107], Eqn (4.21) yields the following equations for the vectors $\mathbf{u}_l$ and $\mathbf{u}_\tau$:

$$\frac{\partial^2 \mathbf{u}_l}{\partial t^2} = c_l^2\Delta\mathbf{u}_l - \frac{K\Omega}{\rho}\,\mathrm{grad}\,n\,, \qquad \frac{\partial^2 \mathbf{u}_\tau}{\partial t^2} = c_\tau^2\Delta\mathbf{u}_\tau\,. \quad (4.24)$$

The solution to the system of equations (4.24) is

$$\mathbf{u}_j = \left[\mathbf{B}\exp(-\varkappa_j z) + \delta_{j,1}\,\mathbf{D}\exp(-\delta_0 z)\right]\exp(\mathrm{i}\kappa x + \gamma t), \quad (4.25)$$

where $j = l, \tau$; $\delta_{j,1} = 0$ if $j = \tau$; $\delta_{j,1} = 1$ for $j = l$; $\varkappa_{\tau,1} = \kappa^2 + \gamma^2/c_{\tau,1}^2$.

Substitution of expressions (4.23) and (4.25) into the boundary conditions given by this set of expressions (4.22) leads to a system of linear algebraic equations. The condition of existence of a nontrivial solution to this new system yields the following dispersion equation for the RD instability on the surface of a semi-infinite medium:

$$(\varkappa_\tau^2 + \kappa^2)^2 - 4\kappa^2\varkappa_l\varkappa_\tau = \frac{D\gamma^2 W\left[(\varkappa_\tau^2+\kappa^2)^2 - 4\kappa^2\varkappa_\tau\delta_0\right]}{\gamma^2 D^2\alpha_0\delta_0 + c_l^2(W - D\alpha_0\delta_0)(\gamma+\beta_0)}\,, \quad (4.26)$$

where the external pump parameter W is given by the expression

$$W = \frac{\beta_0 n_0 K\Omega\Theta}{kT\rho c_l^2}\,.$$

The left-hand side of Eqn (4.26) is a Rayleigh determinant, which governs the law of dispersion of free surface acoustic waves [107]; the right-hand side is related to laser generation of defects.

The structure of Eqn (4.26) is identical with the structure of the dispersion equation for the electron–deformation instability considered in Ref. [96]. It has three types of solution describing three qualitatively different types of an instability:

(a) if the viscosity is taken into account [by replacing $c_{l,\tau}^2$, in Eqn (4.26) with $c_{l,\tau}^2(1 + \eta_{l,\tau}\gamma/\rho c_{l,\tau}^2)$, where $n_\tau = \eta$, $\eta_l = 4\eta/3 + \zeta$, η and ζ are the first and second viscosity coefficients], the dispersion equation (4.26) describes laser generation of surface acoustic waves: $\gamma = \gamma_1 + \mathrm{i}\gamma_2$, $\gamma_1 > 0$, $\gamma_2 \gg \gamma_1$;

(b) an instability of the acoustic wave frequency is characterised by $\gamma_1 < 0$, $\gamma_2 \to 0$;

(c) generation of ordered surface structures ($\gamma_1 > 0$, $\gamma_2 = 0$).

Eqn (4.26) leads to the dispersion equation for static structures [on condition that $\gamma/c_{l,\tau} \ll 1$, $(\gamma+\beta_0)/D\kappa^2 \ll 1$] in the form ($\gamma_1 = \gamma$):

$$\gamma = \frac{2W\kappa}{\alpha_0} - 2D\kappa^2 - \beta_0\,.$$

The maximum increment corresponds to the wave vector $\kappa = \kappa_m = W/2D\alpha_0$ and the value of this increment is $\gamma_m = 2D\kappa_m^2 - \beta_0$. The critical value of the pump parameter is found from the condition $\gamma = 0$: $W_* = \alpha_0(2D\kappa^2 + \beta_0)/2\kappa$. Near the instability threshold $W = 1.1W_*$ and $D = 10^{-6}$ cm^2 s^{-1}, $\kappa_m = 6\times10^4$ cm^{-1}, $\alpha_0 = 10^4$ cm^{-1}, $K = 10^{11}$ erg cm^{-2}, $T = 10^3$ K, the increment is estimated to be $\gamma_m = 10^3$ s^{-1}. The critical vacancy concentration is $n_* = 10^{19}$ cm^{-3}.

It therefore follows that the development of the RD (as well as DD) instabilities on the surfaces of solids leads, in the linear regime, to the formation of a one-dimensional lattice of the defect concentration and the paired lattice of strains. The period of the lattice with the maximum increment γ_m is $d = 4\pi kT\alpha_0/\rho_d n_0\Theta\Omega$. The reduction in d with increase in temperature is related to an increase in the equilibrium defect concentration [$n_0 = \exp(-E_f/kT_0)$].

In addition to one-dimensional (or two-dimensional) lattices, when the RD or DD instabilities appear, structures in the form of radial rays may appear on the surface of a solid. The dispersion equation for these structures is still Eqn (4.26), but subject to the replacement $\kappa^2 = 4m/r_0^2$.

By this means for both the DD and RD instabilities the relationships between the type of the surface structure and the spatial characteristics of laser radiation are similar. The differences are found in the dependences of the parameters of the resultant structures on the specific factors and in the time-dependent characteristics of the laser radiation. All this confirms that it should be possible to control the formation of structures (including quite complex ones) by varying the laser radiation parameters.

4.3 Temporal dissipative structures

Laser irradiation may reveal not only spatial structures but also temporal dissipative structures of the temperatures and concentrations of the interacting particles (self-oscillations). These structures have been investigated actively in recent years for systems of excitons [108], for a plasma [109], and for semiconductors [110]. The appearance of self-oscillations of the temperature and of the concentration of point defects in an irradiated crystal is due to nonlinear feedback between the recombination rate and the temperature of a solid [111]. Irradiation establishes definite quasiequilibrium distribu-

tions of the temperature and defect concentration. A fluctuation-induced increase in temperature enhances the processes of annihilation and energy transfer to the lattice, which in turn increases its temperature. Then the defect concentration falls, the rate of annihilation and temperature decrease, the number of defects rises again, and the process is repeated.

Let us consider the appearance of self-oscillations in a thin crystalline plate cooled in a thermostat where the temperature is maintained at T_i. Let us assume that this plate is subjected to irradiation which creates point defects (specifically, vacancies) at a rate $\mathcal{G}$ which is independent of time and of the spatial coordinate. If a thermal equilibrium is established in a crystal (thermal relaxation time $t_\chi = h^2/\chi$) much faster than an equilibrium of a crystal in the thermostat ($t_i = h\varkappa/b\chi$), i.e. if $t_\chi \ll t_i$ or $h \ll \varkappa/b$, where b represents the exchange of heat with the thermostat, we can assume that both the defect concentration and temperature are distributed homogeneously over the plate. Under these assumptions, it follows from the general model of the CST instability (neglecting the deformation effects) that

$$\frac{\mathrm{d}n}{\mathrm{d}t} = \mathcal{G} - \beta(T)n\,,$$
$$C\rho\,\frac{\mathrm{d}T}{\mathrm{d}t} = Q + E_\mathrm{f}\beta(T)n - \frac{2b(T_i - T)}{h}\,. \qquad (4.27)$$

The system of equations (4.27) has a stationary solution described by the following relationships

$$\mathcal{G} = \beta(T_0)n_0\,, \qquad \frac{(Q + E_\mathrm{f}\mathcal{G})h}{2b} = T_0 - T_i\,. \qquad (4.28)$$

A linear analysis of the stability of the stationary state, described by expression (4.28), against temporal fluctuations proportional to $\exp(\gamma t)$ gives the following dispersion equation for γ [111]:

$$\gamma^2 + A\gamma + B = 0\,,$$

where

$$A = \frac{2b/h + C\rho\beta - \mathcal{G}E_\mathrm{f}E_\mathrm{m}/kT_0^2}{C\rho}\,, \qquad B = \frac{2b\beta}{h}\,.$$

We can easily see that if $\mathcal{G} \to \infty$, $T \to \infty$, then all the real values $\mathrm{Re}(\gamma)$ are negative and the stationary solution is stable. However, if $\mathcal{G} < \mathcal{G}_* = (2b/h + C\rho\beta)kT_0^2/E_\mathrm{f}E_\mathrm{m}$ the solution of the system of equations (4.27) represents a limit cycle with the period $2\pi/\mathrm{Im}(\gamma)$. Self-excited relaxation then appears in the system and the vacancy concentration and temperature of the medium oscillate.

Self-oscillations appear in such a system when the pumping rate is on the order of 10^{17}–10^{18} cm^{-3} s^{-1} at room or lower temperatures. The amplitudes of the temperature and defect concentration oscillations are, respectively, ~ 10 K and 50% of the average value. The frequency of the oscillations is $\omega = 1$–10 s^{-1} [111]. An increase in the concentration of the sinks reduces the instability range and increases the oscillation frequency. If a crystal contains both vacancies and interstitial atoms, a strong dependence of the size of the instability region on the difference between the defect migration energies is observed [111]. The instability region is widest if the ratio of the two energies is unity and it disappears completely when this ratio is on the order of several units.

The role of various traps is considered additionally in Ref. [112]: these traps are present in real crystals and they are capable of trapping point defects, thus forming complexes with vacancies or interstitial atoms. These complexes can act as effective centres of annihilation of vacancies and interstitial atoms. It has been pointed out that the temperature of the appearance of self-oscillations, compared with 'pure' crystals, increases from 300 K to 700 K [112].

In crystals containing impurities we can expect positive feedback to appear as follows: if the temperature increases as a result of a fluctuation, complexes become dissociated liberating some of the defects trapped at sinks and this increases the annihilation rate and temperature. The period of self-oscillations is then considerably greater ($\sim 10^2$ s) and the range of their existence is wider. This wider range is due to the possibility of defect accumulation as a result of complex formation and an increase in the energy stored by defects.

The temporal dissipative structures may be controlled by additional modulation of some system parameters.

5. Spatial extended-defect structures

5.1 Clusterisation of point defects

Laser irradiation can also result in threshold formation of point-defect clusters (pores, dislocation loops of various types, etc.) and also of ordered structures (superlattices) of extended defects in the bulk and on the surface of a solid.

A considerable amount of information on three-dimensional defects formed by irradiation with high-energy particles had been available before laser investigations [113]. Vacancy pores, representing vacancy clusters of size amounting to tens of nanometres, cause radiation swelling of various pieces of equipment operating in the active zones of nuclear reactors.

Clusterisation of defects of one type (vacancies, interstitial atoms, impurity atoms) into vacancy pores and dislocation loops can be treated as the DD instabilities of a homogeneous state of a system of point defects [106]. Within the framework of a general system of CST instabilities , the application of the divergence operation to both parts of Eqn (3.5), carried out on the assumption of adiabaticity of the strain field, gives

$$\mathrm{div}\,\mathbf{u} = K\Omega n\,. \qquad (5.1)$$

Then, subject to Eqn (5.1), it follows from Eqn (3.2) that the diffusion flux of defects is

$$\mathbf{j} = -D\left(1 - \frac{\Omega^2 Kn}{kT}\right)\nabla n\,. \qquad (5.2)$$

Inclusion of the elastic deformation effects gives rise to an additional term in the above expression and it represents the flux opposite to the usual diffusion in a system with defects of the same type ($\Omega^2 > 0$ for $\Omega > 0$ and $\Omega < 0$). In the case of defects of different types ($\Omega_\mathrm{i}\Omega_\mathrm{v} < 0$) the additional flux has the same direction as the diffusion flux. The defects with $\Omega < 0$, for example, vacancies or small-radius impurity atoms, compress the lattice (reduce the volume) and the compressed regions attract defects with $\Omega < 0$ and repel those with $\Omega > 0$.

The quantitative conditions for the appearance of clusters in a system of defects of the same type, for example, vacancies, can be found by substitution of Eqn (5.2) into Eqn (3.1), and linearisation of the latter in the vicinity of the homogeneous

solution ($n_0 = \mathcal{G}/\beta_0$). The instability increment is then

$$\gamma = -D\kappa^2\left(1 - \frac{\Omega^2 K n_0}{kT}\right) - \beta_0 .$$

It therefore follows that the system is unstable if

$$\mathcal{G} > \mathcal{G}_* = \frac{kT\beta}{\Omega^2 K}, \qquad \kappa^2 D > \frac{\beta_0 kT}{\Omega^2 K n_0} . \tag{5.3}$$

Physically, the above conditions are equivalent to a local change in the sign of the effective vacancy diffusion coefficient. This means that the homogeneous distribution of vacancies becomes unstable beginning from a certain critical rate of their formation, which is governed by the temperature of a solid, the dilatation volume of a defect, the bulk modulus, and the concentration of sinks. A directional flux appears and this flux increases the vacancy concentration in the compressed region, causing supersaturation with vacancies and formation of pores.

We shall now consider the nonlinear instability regime. Then, it follows from Eqns (3.1) and (3.5) that the steady Fourier amplitudes of unstable modes are [114]

$$n_\kappa = \frac{n_0 DK\Omega\kappa^2}{kT(D\kappa^2 + \beta_0)\sqrt{\beta_a}}\sqrt{\frac{D\kappa^2 n_0}{(D\kappa^2 + \beta_0)n_*} - 1} , \tag{5.4}$$

$$\varepsilon_\kappa = -\frac{1}{\sqrt{\beta_a}}\sqrt{\frac{D\kappa^2 n_0}{(D\kappa^2 + \beta_0)n_*} - 1} , \tag{5.5}$$

where β_a is the anharmonic constant. Summation of the quantities (5.4) and (5.5) in terms of κ and the assumption (for the sake of clarity) that $\beta_0 = 0$, gives the composite fields of n and ε:

$$n(\mathbf{r}) = n_0\left(1 + \frac{K\Omega}{8\pi^3 kTN_0\sqrt{\beta_a}}\right)\left(\frac{n_0}{n_*} - 1\right)^{1/2}\delta(\mathbf{r}) , \tag{5.6}$$

$$\varepsilon(\mathbf{r}) = -\frac{1}{8\pi^3 N_0\sqrt{\beta_a}}\left(\frac{n_0}{n_*} - 1\right)^{1/2}\delta(\mathbf{r}) . \tag{5.7}$$

Here, N_0 is the number of lattice sites and $\delta(\mathbf{r})$ is the delta-function.

It is evident from expressions (5.6) and (5.7) that the process of formation of defect clusters can be regarded as a second-order nonequilibrium phase transition. It occurs when the rate of generation of defects exceeds the critical value $\mathcal{G}_*$. Typical values of the critical parameters at $T = 700°C$ are $\mathcal{G}_* = 10^{20}$ cm^{-3} s^{-1} and $\kappa_*^2 = 5 \times 10^7$ cm^{-2}.

This mechanism of the appearance of clusters is clearly analogous to the formation of a polaron representing a self-trapped electron state in ionic crystals [115]. The DD instability causes self-trapping of point defects in the potential wells created by the defects themselves.

This approach can also be used in an analysis of the mechanisms of forming the clusters of other point defects, for example, interstitial and impurity atoms [106].

5.2 Pore superlattices

Spatial ordering of pores, giving rise to one-dimensional lattices, concentric rings, and three-dimensional pore superlattices, may occur in a solid at certain laser radiation intensities (or high rates of point defects generation and also when the concentration of pores of certain size is sufficiently high). Pore structures may contain various imperfections, similar to point and linear defects in the crystal lattice (for example, these structures may contain analogues of vacancies and edge dislocations [116]). The symmetry and crystallographic axes of the pore structures are identical with those of the host crystal lattice.

The presence of pore superlattices alters the mechanical [117], optical [116], and superconducting [118] properties of metals. A detailed investigation [118] of superconductors with pore superlattices, subjected to a magnetic field, show that under certain conditions one may observe the Josephson effects associated with the tunnelling of the Cooper pairs between the pores.

The ordering of pores in the form of concentric rings, resulting in a periodic surface relief, was observed in a molybdenum film when it was irradiated with cw CO_2 laser radiation [77]. This was interpreted in Ref. [77] as a pore–deformation instability, analogous in many respects to the DD instability.

A pore superlattice in the bulk of a solid irradiated with nitrogen ions was first observed in 1971 by Evans in pure molybdenum [86]. The temperature of molybdenum was $T = 870°C$ and the energy of the nitrogen ions was 2 MeV. Subsequently, the same effect had been observed in other metals such as aluminium, tungsten, nickel, and niobium [116]. The size of the pores in a superlattice was 2–4 nm and the superlattice period comprised 20–60 nm.

Various theories have been put forward to account for the formation of pore superlattices. The theories have been based on the following: (a) minimisation of the binding energy between ordered pores or minimisation of the configurational energy of the system; (b) anisotropy of the elastic constants of the host crystal limiting pore growth, so that a pore superlattice is matched coherently to the host crystal lattice; (c) quantum fluctuations of the charge density on the surface of ordered pores; (d) stabilisation of a superlattice because of the interaction between the irradiation-generated diffusion fields or fields of stresses around each of the pores [116, 119]. However, the attempts to link the formation of superlattices to some of their properties or to the properties of a crystal have been unsuccessful.

Pore superlattices can be regarded quite rightly as open nonequilibrium dissipative structures [120–123].

The general picture of self-organisation of the pore lattice can be described as follows. Vacancies and interstitial atoms form in the bulk of a solid as a result of irradiation. The latter move faster and can reach the surface joining there other defects. As the number of vacancies increases because of supersaturation of the solution, the process of condensation begins: pores are formed. Vacancies become attached to pores and pores grow. This flux of vacancies to the pores balances out their formation in the bulk. When the radiation intensity is increased, a rise in the number of vacancies should be compensated by an increase of their flux to the pores. This flux is governed by the surface area and also by the spatial distribution of the pores. It becomes maximal as a result of pore ordering. Here, we have a direct analogy with the formation of the Bénard cells [124] in a liquid layer when the motion of particles becomes ordered and this motion ensures an increase in the transmissivity of a liquid when heat is transferred. A necessary condition for positive feedback is then a nonlinear dynamic interaction of a system of pores with point defects.

The state of a system of vacancy pores and vacancies is described by the following equations [121]:

$$\frac{\partial R}{\partial t} = D\Omega\,\frac{n - n_{\rm eq}^s(R)}{R} + D_0(R)\Delta R\,, \tag{5.8}$$

$$\frac{\partial n}{\partial t} = \mathcal{G} - 4\pi DN\Omega R\left[n - n_{\rm eq}^s(R)\right] - D\rho_{\rm d}(n - n_{\rm eq}) + D\Delta n\,, \tag{5.9}$$

where R is the mean radius of a pore; $n_{\rm eq}^s(R) = n_{\rm eq}\exp(2\Gamma\Omega/RkT)$ is the density of the vacancy 'gas' which is in equilibrium with a pore of radius R; $n_{\rm eq}$ is the equilibrium concentration of vacancies; Γ is the surface tension of a crystal; N is the pore concentration; $D_0(R)$ is the pore diffusion coefficient. If it is assumed that pore diffusion is induced by bulk diffusion of point defects, the coefficient $D_0(R)$ can be described by $D_0(R) = D_0/R^2$, $D_0 = 3\Omega D n_{\rm eq} d^2/8\pi$ [125].

The system of equations (5.8) and (5.9) has a quasistationary spatially homogeneous solution (n_0, R_0) described by the following expressions:

$$\mathcal{G} = 4\pi DN\Omega R_0\left[n_0 - n_{\rm eq}^s(R_0)\right] + D\rho_{\rm d}(n_0 - n_{\rm eq})\,,$$

$$R_0\,\frac{{\rm d}R_0}{{\rm d}t} = D\Omega\left[n - n_{\rm eq}^s(R_0)\right]. \tag{5.10}$$

Application of a standard procedure gives the dispersion equation [120] and an analysis of this equation shows that if

$$\rho_{\rm d} \ll \rho_{\rm v} = 4\pi NR_0\,, \qquad \mathcal{G} < \mathcal{G}_* = \frac{2\Gamma\Omega D\rho_{\rm v} n_{\rm eq}^s}{R_0 kT}\,, \tag{5.11}$$

the homogeneous state is unstable: there is a range of values of the wave vector $\kappa_{\rm c(-)}^2 < \kappa^2 < \kappa_{\rm c(+)}^2$, where

$$\kappa_{\rm c(\pm)}^2 = \left\{\Omega(\mathcal{G}_* - \mathcal{G}) + D_0\rho_{\rm v}^2 \pm \sqrt{\left[\Omega(\mathcal{G}_* - \mathcal{G}) + D_0\rho_{\rm v}^2\right]^2 - 4\rho_{\rm v}^2 D_0\Omega(\mathcal{G} + \mathcal{G}_*)}\right\} \times (2D_0\rho_{\rm v})^{-1} - \rho_{\rm v}\,,$$

in which the instability increment $\gamma(\kappa) > 0$, i.e. a homogeneous distribution of pores is unstable when pore lattices are formed. The maximum increment and the maximum wave number are [120]

$$\gamma_{\rm m} = \frac{\Omega(\mathcal{G}_* - \mathcal{G}) - 2\rho_{\rm v}\sqrt{\Omega(\mathcal{G} + \mathcal{G}_*)/D_0}}{\rho_{\rm v}R_0^2} + \frac{D_0\rho_{\rm v}}{R_0^2}\,,$$

$$\kappa_{\rm m}^2 = \sqrt{\frac{\Omega(\mathcal{G} + \mathcal{G}_*)}{D_0}} - \rho_{\rm v}\,.$$

For typical values of the constants $N = 10^{16}$ cm^{-3}, $D = 10^{-6}$ cm^2 s^{-1}, $R_0 = 10$ nm at $T = 700$°C, the instability growth time is $t = \gamma_{\rm m}^{-1} = 10$ s, i.e. pore superlattices can form under the action of cw laser radiation.

If at the initial stage of the process of superlattice formation the pores are distributed at random and there is no pore lattice, then when pores reach such dimension and concentration that the conditions (5.11) are satisfied, a kinetic phase transition occurs in the system: a homogeneous pore distribution becomes inhomogeneous and a periodic structure appears with a characteristic scale

$$d = \frac{2\pi}{\left[\sqrt{(\mathcal{G} + \mathcal{G}_*)/D_0} - \rho_{\rm v}\right]^{1/2}}\,. \tag{5.12}$$

It follows from formula (5.12) that the superlattice period rises with increase in temperature and decreases with increase in the pumping rate. An estimate based on this formula gives the period $d = 40$ nm.

The model of self-organisation of pore lattices accompanied by simultaneous generation of vacancies and interstitial atoms was considered in Refs [122, 123].

5.3 Dislocation lattices

Formation of periodic dislocation structures has been observed under various conditions and for various materials. The appearance of a dislocation lattice on a silicon plate under the action of continuous but scanning CO_2 laser radiation is reported in Refs [104, 126] and a similar effect of millisecond laser pulses is described in Ref. [87]. The process has a threshold and is observed at sufficiently high dislocation densities ($\rho_{\rm d} > \rho_{\rm d*} = 10^8$ cm^{-2}). The period of these structures is 1 – 10 μm [87, 104].

The appearance of a dislocation lattice as a result of action of laser radiation on the surface of a crystal is a self-organisation process due to positive feedback between the stress acting on a dislocation and its velocity [95]: $v = V_0(\sigma_{ii}/E)^n$, where n and V_0 are the constants of the material. Formation of a dislocation lattice as a result of development of an intraplane dislocation – deformation instability will be discussed on the basis of the simplest model. It is assumed that there is a system of randomly distributed edge dislocations with the Burgers vector **b**. These dislocations are parallel to the Oz axis and in the xOy plane (glide plane) their density is $\rho_{\rm d}$. All the dislocations are assumed to be the same. The problem is essentially one-dimensional: $\rho_{\rm d} = \rho(x)$, $u_z = u_z(x)$. The main processes controlling the time dependence of the dislocation density are taken into account: they are the motion along the x axis as a result of diffusion and drift [95], and also generation of dislocations and their mutual annihilation. The development of an instability is then described by a system of equations for the dislocation density and the strains in the investigated medium:

$$\frac{\partial\rho}{\partial t} = -\frac{\partial j_{\rm d}}{\partial x} + \alpha_{\rm d} v\rho - \beta_{\rm d} v\rho^2\,, \quad j_{\rm d} = -D_{\rm d}\,\frac{\partial\rho}{\partial x} + v\rho\,, \tag{5.13}$$

$$\frac{\partial^2 u_z}{\partial t^2} = c_\tau^2\,\frac{\partial^2 u_z}{\partial x^2} + c_\tau^2\beta_{\rm a}\,\frac{\partial^2 u_z^3}{\partial x^2} + bc_\tau^2\rho\,, \tag{5.14}$$

where $D_{\rm d}$, $\alpha_{\rm d}$, and $\beta_{\rm d}$ are, respectively, the dislocation diffusion, generation, and annihilation coefficients.

Substitution of $\rho = \rho_0 + \rho_1$, $u_z = u_{z0} + u_{z1}$ into Eqns (5.13) and (5.14) (here, ρ_0 and u_{z0} are the average homogeneous values and ρ_1 and u_{z1} are small deviations) and linearisation of these equations gives a system of equations the solution of which can be written in the form

$$u_{z1} = a_\kappa\exp({\rm i}\kappa x + \gamma t)\,, \qquad \rho_1 = b_\kappa\exp({\rm i}\kappa x + \gamma t)\,, \tag{5.15}$$

where a_κ and b_κ are the amplitudes of the Fourier harmonics.

The dispersion equation is then obtained in the form (on the assumption that $\kappa^2 c_\tau^2 \gg \gamma^2$)

$$\gamma = -D_d\kappa^2 + bg - \beta_d v_0\rho_0\,, \qquad g = \frac{\rho_0 v_0}{\varepsilon_0}\,,$$

which generalises the corresponding equation given in Ref. [95].

The instability conditions are

$$bg > \beta_d v_0\rho_0\,, \qquad 0 < \kappa^2 < \kappa_0^2 = \frac{bg - \beta_d v_0\rho_0}{D_d}\,.$$

The resultant instability becomes stabilised because of the anharmonicity of the elastic continuum [95]. It follows from Eqns (5.13) and (5.14) that the steady amplitude of the Fourier harmonics is

$$a_\kappa = \left(\frac{\kappa_0^2/\kappa^2 - 1}{\beta_a}\right)^{1/2}.$$

The resultant deformation pattern is obtained by substituting a_κ into the set of expressions (5.15), where $\gamma = 0$, and summing the Fourier harmonics with the wave vectors $\kappa \leqslant \kappa_0$:

$$u_z = \sum_\kappa a_\kappa \exp(i\kappa x) \sim \int_0^\kappa \kappa\left(\frac{\kappa_0^2}{\kappa^2} - 1\right)^{1/2}\cos(\kappa x)\,d\kappa \sim J_1(\kappa_0 x)\,.$$

The dislocation lattice period is

$$d = 2\pi\left(\frac{D_d}{bg - \beta_d v_0\rho_0}\right)^{1/2}.$$

The mechanism of dislocation ordering associated with the development of an interplanar dislocation–deformation instability under the influence of cw laser radiation is considered in Ref. [104]. A spatial Fourier harmonic of the dislocation density in a medium (substrate), which appears as a result of fluctuations, generates — at the interface with the film — a harmonic of a stress perpendicular to the film. This causes flexural deformation of the film and leads to a further redistribution of the dislocation density because of the deformation-induced vacancy drift. If the dislocation density exceeds the critical value, $\rho > \rho_{d*} = D_d\kappa h_0^3/24A$ (where $A = \Theta_v\Theta_d h_0^2 D_d/4\mu kT$, $D_d = D_v n_v\Omega$; Θ_v and Θ_d are the deformation potentials of vacancies and dislocations, respectively, and h_0 is the length of a dislocation), the initial fluctuations of the dislocation density begin to grow in time and this leads to an instability accompanied by the formation of a periodic structure of dislocations with a period $d \approx kT/K\rho_0 d_0^4$. This model is in agreement with the results of experiments [104].

The formation of dislocations on the surface of sample occurs because of considerable thermal strains resulting from the transient and inhomogeneous nature of the temperature field in the irradiation zone. Therefore, a change in the spatial–temporal distribution of the temperature field in this zone can be used to control the formation of a dislocation lattice in a solid. Creation of a suitable temperature field can reduce considerably the dislocation density and, under certain conditions, laser irradiation can prevent completely the formation of dislocations.

6. Instabilities in melts exposed to laser radiation

6.1 Formation of a liquid phase. Deep penetration melting

When solids are subjected to laser radiation with a photon flux exceeding the melting threshold $I \geqslant I_{melt}$ (the range of I_{melt} for a pulsed laser emitting pulses of $\tau \geqslant 1$ ms duration is $\approx 10^4 - 10^5$ W cm^{-2} [6]), a phase transformation takes place: a molten layer forms on the irradiated surface. In some of the technological processes a region occupied by the melt has a depth of 200–300 μm and a diameter 1–2 mm. A further increase in the radiation intensity results in intensive evaporation of the material. Much experimental work has been done on the temperature distributions, transport processes, and velocity fields in melts under different laser irradiation conditions [6, 127]. The presence of a liquid phase provides new opportunities for the control of the processes which then occur. For example, capillary and thermocapillary effects, which have a significant influence on the efficiency of absorption of the incident energy [5, 6], occur during laser irradiation and the processes resulting in the absorption of gases from the surrounding medium and mixing of convective fluxes make it possible to control the composition of the surface layer of the melt and to induce an anomalously rapid redistribution of impurities in the course of metal doping [5].

In the irradiation zone when a liquid phase is present, we can expect formation of a deep vapour–gas crater with a large (on the order of 10–30 [128]) depth-to-diameter ratio of the molten region. This effect is known as deep penetration (or 'keyhole') melting and it is affected critically by the laser radiation flux. If $I > I_{dpm}$ (I_{dpm} is the deep penetration melting threshold), the molten zone grows strongly and the melt partly evaporates. Under the influence of the pressure of the vapour leaving the molten surface the liquid metal is pushed out from the focal spot region. The melt surface is strongly deformed and assumes a shape elongated in the direction of the beam. This deepens the zone of absorption of the radiation and enhances the heating of deeper layers of matter. Typical values of I_{dpm} obtained for a focal spot radius of 10^{-2} cm amount to $\approx 10^5$ W cm^{-2} for low-melting-point metals and $\approx 10^6$ W cm^{-2} for refractory metals [146].

Various surface (capillary, thermocapillary, evaporation) waves may form on the free surface of the melt both as a result of surface processing accompanied by melting and in the course of formation of a vapour–gas crater [129–156]. These waves appear in a wide range of the laser radiation parameters ($\lambda = 0.308 - 10.6$ μm, pulse duration $\tau = 10$ ps–1 ms, and intensity $I = 10^5 - 5 \times 10^8$ W cm^{-2}) and for melts formed from different materials. The first irreversible (solidified after the end of a pulse) periodic structures of the surface relief were observed on irradiation of the surface of molten Si and Ge with ruby laser pulses [132]. This was followed by observations on melts of different metals [133, 134] and insulators [135–139]. A strong correlation of the parameters of these structures with the laser radiation characteristics (polarisation, frequency, energy) makes it possible to speak of 'laser-induced capillary waves' [129].

Ref. [143] gives data on the formation of cellular (10 μm in diameter) and filamentary (with a period of 0.1 μm) surface structures on molten Si and Ge subjected to picosecond pulses. The parameters of these structures are practically independent of the polarisation and angle of incidence of

radiation, but are governed by the intensity and duration of laser irradiation.

Experimental results reveal both low-frequency ($10-10^2$ Hz) and large-scale ($10^{-2}-10^{-1}$ cm), as well as high-frequency (10^3-10^5 Hz) and small-scale ($10^{-3}-10^{-5}$ cm), waves. High-frequency oscillations in a vapour–gas crater cause periodic ejection of a vapour associated with an erosion or plasma jet [156].

Build-up of surface perturbations may alter significantly the conditions governing the reflection and absorption of light on the surface of a melt and can influence the processes of heat and mass transfer in a liquid. For example, experimental observations are reported [140, 141] of an increase in the absorptivity as a result of appearance of surface lattices with a period $d \approx \lambda$. An increase in the efficiency of energy deposition in a vapour–gas crater as a result of formation of spatially periodic structures on its walls is mentioned in Ref. [5]. When large-scale oscillations of the melt surface (with an amplitude on the order of the crater diameter) appear, the melt material at the crests of the capillary waves is no longer held back by the surface tension forces and becomes detached from the melt surface in the form of microdroplets. These droplets begin to evaporate in a laser radiation field. The result is an additional pressure on the melt surface, causing enhancement of mass transfer in the crater [153]. The appearance of thermocapillary vortex motion in the subsurface layer of a melt creates conditions under which some of the free energy of the system may be converted into the kinetic energy of convective motion in the liquid, which in its turn increases heat transfer to the liquid phase and accelerates the phase transformation on the surface [144].

It therefore follows that, from the point of view of feasibility of controlling various thermophysical processes (such as melting, evaporation, hydrodynamic phenomena in a melt, etc.) in the irradiation zone, it is very important to identify and to know the quantitative conditions for the activation of these regimes as a function of the radiation parameters and of the properties of the medium.

A special role in the excitation of surface waves is played by instabilities that appear in the course of the interaction of laser radiation with the surface of a melt.

6.2 Thermocapillary instability

At moderate values of the laser radiation intensity, $I = 10^4-10^5$ W cm^{-2}, when evaporation from the melt surface is slight, a thermocapillary (TC) instability may appear because of the action of TC forces along the free surface (these forces are due to spatial and temporal modulation of the surface tension σ through the modulation of the temperature on the irradiated surface) and also because of the presence of a high steady temperature gradient in the surface layer [131, 144, 145]. When fluctuations are induced along the free surface of a melt and the melt is incompressible, the liquid is set in motion in transverse direction and this creates crests and valleys on the melt surface. If there is a constant negative transverse temperature gradient in the surface layer, the surface temperature rises at the crests and decreases in the valleys. An inhomogeneous temperature field created in this way generates forces $F_z = -\mathrm{grad}\,\sigma$ which are directed from the hotter to the colder regions. These forces act on the surface layer and set it in motion: they create a depression, i.e. the liquid surface becomes bent in the regions where the temperature is higher. Then, under suitable external conditions, small hydrodynamic and thermal fluctuations, as well as fluctuations of the shape of the free surface, begin to grow without limit thus leading to an instability.

A model of the TC instability on a flat surface proposed in Refs [131, 144] deals with a viscous liquid. It is assumed that in the state of rest this liquid occupies a layer $0 > z > -h$ and that the heat flux Q is absorbed uniformly on its free surface $z = \xi(x)$. Under steady-state conditions, we have

$$\xi(x) = 0\,, \qquad \frac{\mathrm{d}T_0}{\mathrm{d}z} = \frac{Q}{\varkappa}\,.$$

Linearisation, relative to this steady state, of the Navier–Stokes equations as well as of the continuity and heat conduction equations, yields the following system of equations [144]:

$$\Delta\Phi = 0\,, \qquad \frac{\partial \mathbf{A}}{\partial t} = \nu\Delta\mathbf{A}\,, \qquad \mathrm{div}\,\mathbf{A} = 0\,,$$

$$\frac{\partial T}{\partial t} - \chi\Delta T = -V_z\,\frac{\mathrm{d}T_0}{\mathrm{d}z}\,, \qquad V = \nabla\Phi + \mathrm{curl}\,\mathbf{A} \tag{6.1}$$

subject to the boundary conditions on the free surface ($z = 0$)

$$\rho\,\frac{\partial^2\Phi}{\partial t^2} = \sigma\Delta V_z - \rho g V_z - 2\eta\,\frac{\partial^2 V_z}{\partial t\,\partial z}\,,$$

$$\sigma_T\,\frac{\partial T}{\partial x} = \eta\left(\frac{\partial V_x}{\partial z} + \frac{\partial V_z}{\partial x}\right).$$

At $z = -h$, we have $T = \mathrm{const}$ and $V = 0$.

Here, Φ and $\mathbf{A}$ are the scalar and vector velocity potentials; $\sigma_T = -\mathrm{d}\sigma/\mathrm{d}T_0 > 0$ is the temperature coefficient of the surface tension; g is the acceleration due to gravity; ν is the viscosity coefficient; $\Delta = \partial^2/\partial x^2 + \partial^2/\partial y^2$.

The system of equations (6.1) leads to the dispersion equation for the TC instability. In the limiting case of short-wave perturbations (when $\kappa h \gg 1$ and $\chi\kappa^2 \ll \omega_0$), the dispersion equation looks like [144]

$$\gamma = \frac{\sigma_T\kappa^2}{2\sqrt{2}\,\rho\omega_0}\sqrt{\frac{\chi\kappa^2}{\omega_0}}\,\frac{\mathrm{d}T_0}{\mathrm{d}z} - 2\nu\kappa^2\,, \tag{6.2}$$

where $\omega_0^2 = \sigma\kappa^3/\rho + \kappa g$ is the frequency of gravitation–capillary waves.

It follows from Eqn (6.2) that there is a threshold value of the heat flux above which a capillary wave becomes unstable. The minimum threshold corresponds to oscillations characterised by the wave number $\kappa = \kappa_c = (\rho g/5\sigma)^{1/2}$ and frequency $\omega_c = \omega_0(\kappa_c)$, and is equal to

$$Q_c = \frac{4\sqrt{2}\,\varkappa\eta}{\sigma_T}\sqrt{\frac{\omega_c^3}{\chi\kappa^2}}.$$

This TC instability model is generalised to nonplanar phase boundaries in Ref. [145]. In analysis of instabilities in a cylindrical vapour–gas crater a layer of the melt occupying a region $b < r < a(\varphi, z, t)$ is taken into account; here, b and a are the radii of the molten zone and of the crater, respectively. The depth of the molten channel is assumed to be much greater than the inner and outer radii of the melt. A steady state of the melt is described by the formulas

$$V_r = V_\varphi = V_z = 0\,, \qquad \xi(\varphi, z) = 0\,, \qquad P = \mathrm{const}\,,$$

$$T_0(r) = T_e + (T_e - T_m)\,\frac{\ln(r/b)}{\ln(a/b)}\,, \tag{6.3}$$

where V_r, V_φ and V_z are the components of the vector representing the melt velocity; P is the pressure; T_m and T_e are the melting and evaporation temperatures, respectively.

Although because of heat conduction, $T_0(r)$ can vary with time, this variation can be ignored for instabilities characterised by growth times (γ^{-1}) shorter than the characteristic time of a change in $T_0(r)$.

We shall represent a perturbation of the shape of the free surface by

$$\xi(\varphi, z, t) = \xi_0 \exp\left[\gamma t + \mathrm{i}(m\varphi + \kappa z)\right],$$

where ξ_0 is the complex amplitude of the perturbation, and κ and m are the axial and azimuthal wave numbers of the perturbation.

The equations for small perturbations of thermocapillary motion in a crater are of the form [145]

$$\gamma u_1 = -\widehat{\mathrm{D}}p_1 + \left(\widehat{\mathrm{L}}u_1 - \frac{2\mathrm{i}mv_1}{\zeta^2}\right),$$

$$\gamma v_1 = -\frac{\mathrm{i}mp_1}{\zeta} + \left(\widehat{\mathrm{L}}v_1 + \frac{2\mathrm{i}mu_1}{\zeta^2}\right),$$

$$\gamma w_1 = -\mathrm{i}\kappa p_1 + \left(\widehat{\mathrm{L}} + \frac{1}{\zeta^2}\right)w_1,$$

$$\left(\widehat{\mathrm{D}} + \frac{1}{\zeta}\right)u_1 + \frac{\mathrm{i}mv_1}{\zeta} + \mathrm{i}\kappa w_1 = 0,$$

$$\gamma Pr\Theta_1 + G(\zeta)u_1 = \frac{1}{\mathrm{Pe}}\left(\widehat{\mathrm{L}} + \frac{1}{\zeta^2}\right)\Theta_1, \tag{6.4}$$

$$p_1 - 2\widehat{\mathrm{D}}u_1 = \mathrm{Ma}\left[\Theta_1 + G(1)\xi_1\right] - \mathrm{We}(1 - \kappa^2 - m^2)\xi, \tag{6.5}$$

$$\widehat{\mathrm{D}}v_1 + \mathrm{i}mu_1 - v_1 = -\mathrm{i}m\,\mathrm{Ma}\left[\Theta_1 + G(1)\xi\right], \tag{6.6}$$

$$\mathrm{i}\kappa u_1 + \widehat{\mathrm{D}}w_1 = \mathrm{i}\kappa\,\mathrm{We}\left[\Theta_1 + G(1)\xi\right], \tag{6.7}$$

$$\gamma\xi = u_1, \qquad \widehat{\mathrm{D}}\Theta_1 = \xi\frac{\mathrm{d}G}{\mathrm{d}\zeta(1)}\ (\zeta = 1), \tag{6.8}$$

$$u_1 = w_1 = v_1 = 0, \qquad \Theta_1 = 0, \qquad \widehat{\mathrm{D}}\Theta_1 = 0\ \ (\zeta = s). \tag{6.9}$$

Here, $\widehat{\mathrm{L}} = (\widehat{\mathrm{D}} + 1/\zeta)\widehat{\mathrm{D}} - (\kappa^2 + m^2/\zeta^2)$; $\widehat{\mathrm{D}} = \mathrm{d}/\mathrm{d}\zeta$; u_1, v_1, w_1, Θ_1, p_1 are the complex amplitudes of perturbations of the velocity, temperature, and pressure; γ is the dimensionless instability increment; $(\zeta, \varphi, z) = (r/a, \varphi, z/a)$; $s = a/b$; $\tau = tu_0/a$; $p = P/\rho u_0^2$; $u_0 = \nu/a$; $\Theta = \varkappa T/Qa$, $G(\zeta)$ is the dimensionless temperature gradient; $\mathrm{Ma} = \sigma_T aQ/\rho\nu\chi\varkappa$ and $\mathrm{We} = a\sigma/\rho\nu^2$ are the Marangoni and Weber numbers representing the relative role of the thermocapillary and surface tension forces, respectively; $\mathrm{Pe} = u_0 a/\chi$ is the Peclet number.

The conditions (6.5)–(6.7) describe the balance between normal, tangential, and angular tensions on the melt surface. The condition (6.8) takes account for the influence of perturbations of the melt free surface on the heat flow across it. The influence of viscous dissipation is ignored. The first and second boundary conditions in expression (6.9) follow from the adhesion hypothesis and from the equation of continuity.

The condition of existence of a nontrivial solution to the problem described by Eqns (6.4)–(6.9) leads to critical values of the Marangoni number $\mathrm{Ma}(\kappa, m, \mathrm{We})$, which define a neutral stability surface:

$$\mathrm{Ma}(\kappa, m) = \frac{\kappa(1 - \kappa^2 - m^2)S_1}{(1 - \kappa^2 - m^2)E_m + R_m/\mathrm{We}}, \tag{6.10}$$

where

$$S_1 = I'_m(\kappa)K'_m(\kappa s) - K'_m(\kappa)I'_m(\kappa s),$$

$$E_m = \int_1^s \phi(y)\left[I'_m(\kappa s)K_m(\kappa y) - I_m(\kappa y)K'_m(\kappa s)\right]\mathrm{d}y,$$

$$R_m = \left[-f(1) + 2\phi'(1) + 1\right](\kappa S_1 - S_2),$$

$$S_2 = I'_m(\kappa s)K_m(\kappa) - K'_m(\kappa s)I_m(\kappa). \tag{6.11}$$

The functions $\phi(\xi)$ and $f(\xi)$ satisfy the system

$$\widehat{\mathrm{L}}_1\varphi - \frac{2\mathrm{i}m}{\zeta^2}\phi = \widehat{\mathrm{D}}f, \qquad \widehat{\mathrm{L}}\phi + \frac{2\mathrm{i}m}{\zeta^2}\varphi = \frac{\mathrm{i}m}{\zeta}f, \qquad \widehat{\mathrm{L}}f = 0. \tag{6.12}$$

Here, $\widehat{\mathrm{L}}_1 = \widehat{\mathrm{L}} - 1/\zeta^2$; I_m and K_m are Bessel functions of the mth order; a prime denotes differentiation with respect to the radial variable.

We can use expressions (6.10)–(6.12) to calculate the neutral stability curve, the minimal critical Marangoni numbers Ma (or radiation intensities), and the critical wave numbers.

Figure 2 shows typical behaviour of the neutral curves $\mathrm{Ma}(\kappa)$, plotted on the basis of expressions (6.10) and (6.12) for axisymmetric perturbations ($m = 0$) when $s = 3$. Curve *1* represents an undeformable free surface of a melt ($\mathrm{We} = \infty$). The minimal critical number $\mathrm{Ma}_* = 200$ corresponds to $\kappa_* = 0$. If the surface is deformable ($\mathrm{We} \neq \infty$), the neutral stability curve has a singularity and its position depends on We. For example, if $\mathrm{We} = 300$, a graph of $\mathrm{Ma}(\kappa)$ has a vertical asymptote at $\kappa_0 = 1.3$ (curve *2*). For wave numbers in the interval $1 < \kappa < \kappa_0$, we have $\mathrm{Ma}(\kappa) < 0$ and $\mathrm{Ma}(\kappa) \to -\infty$ if $\kappa \to \kappa_0 - 0$. In the interval $0 < \kappa < \kappa_0$ the dependence $\mathrm{Ma}(\kappa)$ reaches its positive maximum $\mathrm{Ma}_{\max} = 180$ at $\kappa < 0.5$; for $\kappa > \kappa_0$, it reaches a positive minimum $\mathrm{Ma}_{\min} = 280$ at $\kappa = 1.6$. When We is reduced, the point of discontinuity (κ_0) shifts to the right, the Marangoni number decreases and, consequently, the stability of the molten layer becomes less. The point of discontinuity approaches unity for $\mathrm{We} \to \infty$. When the wave number κ (or We) is increased, all the $\mathrm{Ma}(\kappa, \mathrm{We})$ curves rapidly approach one another and we have $\mathrm{Ma} \approx 10\kappa^2$ for $\mathrm{We} = \infty$. Similar asymptotic behaviour is predicted also for azimuthal perturbations. It follows from expressions (6.10) and (6.11) that an increase in the layer thickness s enhances the stability

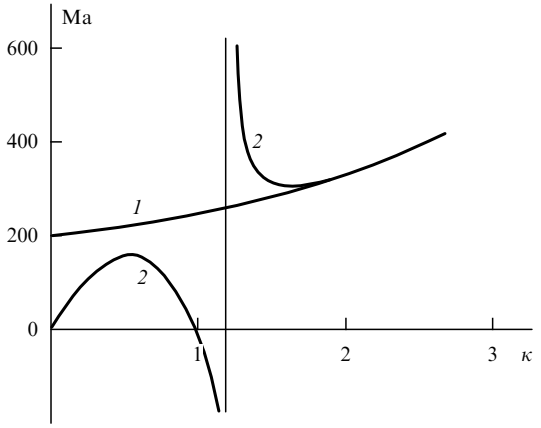

Figure 2. Dependence of the Marangoni number on the wave number for $\mathrm{We} = \infty$ (*1*) and $\mathrm{We} \neq \infty$, $s = 3$ (*2*) [145].

margin. For example, if $s = 3$, we have Ma = 800 for $\kappa = 3$, but if $s = 2$, then Ma = 200 for $\kappa = 4$. If the curvature of the walls of a vapour – gas crater is small (planar molten layer), the critical Marangoni numbers behave asymptotically in the same manner as in the range of short wavelengths. Therefore, for short-wavelength perturbations the critical conditions for the appearance of the TC instability cease to depend on the dimensions and geometry of the region occupied by a liquid.

6.3 Evaporation-capillary instability

Evaporation–capillary (EC) instabilities predominate when the laser radiation intensity is increased ($I > 10^5$ W cm^{-2}). Investigations have been made of the various conditions for evaporation of a planar phase boundary (subsonic [154], evaporation in vacuum or in a medium with a low counter-pressure [5, 131, 146]) and also of specific reasons for the development of these instabilities. For example, a nonlinear coupling between the rate of evaporation and the surface temperature is responsible for an instability of surface evaporation from a thin layer of thickness $\Delta l \ll \alpha^{-1}$ [131, 146]. Since the laser beam energy is released in a certain finite volume near the phase boundary, the temperature distribution maximum shifts from the surface deeper into the material. An accidental displacement of some part of the interface in the direction of the hotter condensed phase increases the heat flux to this region and this enhances the mass flux because of the additional evaporation of matter and, consequently, a depression of the surface becomes even deeper. The resultant spatially periodic structures have a period on the order of the skin-layer depth [5].

An instability of the melt surface in the presence of large-scale perturbations, associated with the nonlinear dependence of the absorption coefficient on the angle of slide, is considered in Ref. [142]. Growth of perturbations is governed by the spatially inhomogeneous evaporation pressure.

A unified approach in used in Refs [129, 130] to consider laser-induced instabilities accompanied by the excitation of surface waves at a plane interface between the phases. The incident laser radiation is diffracted by the Fourier component of the surface relief (initial irregularities). Interference between the pump wave penetrating the medium and the diffracted waves creates a spatially periodic distribution of the laser energy in the subsurface layer. Since absorption takes place, a surface wave of a change in temperature is formed. Consequently, spatially periodic forces (thermocapillary or recoil-pressure forces) appear and they enhance the amplitudes of the 'seed' perturbations. If $I > I_{\text{melt}}$, an instability of capillary waves is observed, but at higher values of I, interference surface – evaporation instabilities are felt.

Interference instabilities are observed under the action of powerful ($I = 10^7 - 10^{10}$ W cm^{-2}) short laser pulses. The growth of these instabilities up to the end of a pulse creates irreversible ordered structures on the melt surface: they are one-dimensional or two-dimensional lattices of the surface relief with a period $d \leqslant \lambda$.

The geometry of these structures depends on the direction of the projection $\mathbf{E}_t$ of the vector representing the intensity of the electric field $\mathbf{E}$ of a wave incident on the planar surface and also on the permittivity of the medium $\varepsilon_d(\omega) = \sqrt{n + i\omega}$. If $|\varepsilon_d| \gg 1$, longitudinal lattices prevail (the wave vector of such lattices is $\mathbf{q} \parallel \mathbf{E}_t$). If $\varepsilon_d \approx 1$, transverse structures are formed ($\mathbf{q} \perp \mathbf{E}$). For the s polarisation of the incident wave, if $|\varepsilon_d| \gg 1$, the longitudinal lattice period is $d \approx \lambda/\cos\vartheta$, whereas for the p polarisation, there are two longitudinal lattices with the periods $d \approx \lambda/(1 \pm \sin\vartheta)$ [129]; ϑ is the angle of incidence of laser radiation. A linear theory of the interference instability is used in Ref. [130] to derive expressions for the increments of the dominant structures as a function of I, ϑ and $\boldsymbol{\kappa}$.

One of the manifestations of this instability during the nonlinear stage is the self-induced increase in the absorptivity of the surface, associated with resonant transfer of energy to the diffracted surface waves. For example, in the case of metals the absorptivity may increase from $A = 10^{-1} - 10^{-2}$ to $A = 1$.

In the general theory of the EC instabilities and of the cylindrical vapour – gas crater, both the axisymmetric and azimuthal perturbations of the melt surface are taken into account [147]. If evaporation has little influence on the overall energy balance and on the unperturbed temperature profile $T_0(r)$ of a melt, the steady state of this melt is described by the set of expressions (6.3).

In the absence of dissipation (inviscid liquid), the field of velocities V in a liquid becomes vortex-free and can be represented by a gradient of the potential function Φ. In the presence of a radial gradient of the unperturbed temperature in a surface layer, the appearance of weak hydrodynamic motion described by the velocity potential Φ leads, because of convection (proportional to the radial component V_r of motion of the melt), to modulation of the temperature for the free surface. Perturbation of the temperature field $T_1(r, z, t) = \Theta(r)\exp\left[\gamma t + i(\kappa z + m\varphi)\right]$ results in a change in the evaporation pressure $\delta P = \varepsilon_T T_0 \exp\left[\gamma t + i(m\varphi + \kappa z)\right]$ ($\varepsilon_T = dP/dT$ is the derivative of the evaporation pressure P with respect to the surface temperature). The force which is then generated ($F \sim \nabla P$) amplifies small perturbations of the surface and leads to an instability.

A system of equations describing the development of the EC instability in a crater reads as follows:

$$\mathbf{u} = \nabla\Phi\,, \qquad \Phi(r, z, t) = \Phi_0\left[I_m(\kappa r) - AK_m(\kappa r)\right] \times \exp\left[\gamma t + i(\kappa z + m\varphi)\right], \tag{6.13}$$

$$\left(\frac{\gamma}{\chi} + \frac{m^2}{r^2} + \kappa^2\right)\Theta - \left(\frac{d^2\Theta}{dr^2} + \frac{1}{r}\frac{d\Theta}{dr}\right) = -\frac{V_r G(r)}{\chi}\,, \tag{6.14}$$

$$\frac{d\Theta}{dr}(r = a) = G'(r = a)\xi\,, \qquad \Theta(r = b) = 0\,, \tag{6.15}$$

$$-\rho\gamma\Phi(r = a) = \sigma(a^{-2} - \kappa^2 - m^2a^{-2})\xi + T_s\varepsilon_T\,, \tag{6.16}$$

$$\gamma\xi = \frac{\partial\Phi}{\partial r}(r = a)\,. \tag{6.17}$$

Eqn (6.13) describes the velocity field; Eqns (6.14) and (6.15) represent the boundary-value problem for the amplitude Θ of the temperature perturbations; expression (6.16) is the hydrodynamic boundary condition reflecting the continuity of the momentum flux at the evaporation front; expression (6.17) is the kinematic condition. Here, $A = I'_m(\kappa b)/K'_m(\kappa b)$, $G(r) = -G_0/r$, $G_0 = (T_{\text{eq}} - T_{\text{m}})/\ln(a/b)$.

A perturbation of the surface temperature $T_s = T(a) + G(a)\xi$ is described by the following expression, deduced from Eqn (6.14) and expressions (6.15) and (6.17) [147]:

$$T_s = G(a)\xi_0\left[\frac{a\gamma}{\chi l_0}(e_1 l_1 - l_2) + \frac{e_1}{qa} + 1\right] \times \exp\left[\gamma t + i(\kappa z + m\varphi)\right]. \tag{6.18}$$

Here,

$$e_1 = \frac{I_m(qa) - SK_m(qa)}{I'_m(qa) + SK'_m(qa)}, \qquad S = \frac{I_m(qb)}{K_m(qb)},$$

$$l_0 = AK'_m(\kappa a) + I'_m(\kappa a), \qquad l_1 = \int_a^b B'(qa, qy)\psi_1(y)\,\mathrm{d}y,$$

$$l_2 = \int_a^b B(qa, qy)\psi_1(y)\,\mathrm{d}y, \qquad \psi_1(y) = I'_m(\kappa y) + AK'_m(\kappa y),$$

$$B(qr, qy) = I_m(qy)K_m(qr) - I_m(qr)K_m(qy), \quad q^2 = \frac{\gamma}{\chi} + \kappa^2.$$

The dispersion equation determines the dependence of the complex EC instability increment γ on the axial and azimuthal wave numbers of perturbations, on the surface temperature (or on the intensity of the laser radiation), on the curvature of the crater walls, and also on the physical properties of the medium [147]. This equation can be deduced from Eqns (6.16)–(6.18):

$$\gamma^2 - \frac{\sigma}{\rho a^2}\kappa(1 - m^2 - \kappa^2 a^2)e_2 = -\left[\frac{a\gamma}{\chi l_0}(e_1 l_1 - l_2) + \frac{e_1}{qa} + 1\right]\frac{\varepsilon_T G \kappa e_2}{\rho}, \tag{6.19}$$

where $e_2 = -l_0\left[I_m(\kappa a) + K_m(\kappa a)A\right]^{-1}$, $A = I'_m(\kappa b)/K'_m(\kappa b)$.

In Eqn (6.19) the right-hand side represents modulation of the surface temperature resulting from perturbation, by a surface wave, of an inhomogeneous (in respect to the radial coordinate) steady temperature distribution in a melt.

For axisymmetric short-wavelength perturbations ($\kappa a \gg 1$, $m = 0$), it follows from Eqn (6.19) that [148]:

$$(\gamma^2 + \omega_0^2)\left(\kappa^2 + \frac{\gamma}{\chi}\right)^{1/2} = -\frac{\varepsilon_T G_0 \kappa^2}{a\rho}, \tag{6.20}$$

where $\omega_0 = (\sigma/\rho)^{1/2}\kappa^{3/2}$ is the frequency of capillary waves in a homogeneous liquid.

The solution of Eqn (6.20), obtained for $(\gamma/\chi\kappa^2) \gg 1$ and $\varepsilon_T G \kappa^2 \chi^{1/2}/\rho \gg \omega_0^{5/2}$, is [148]

$$\gamma \approx \frac{\gamma_0^2 - 2\omega_0^2/5}{\gamma_0}. \tag{6.21}$$

It follows from expression (6.21) that, for waves with the wave numbers in the interval

$$a^{-1} < \kappa < \kappa_1 = \left(\frac{5}{2\sigma}\right)^{5/7}\left(\frac{\varepsilon_T G_0 \chi^{1/2}\rho^{1/4}}{a}\right)^{4/7},$$

the increment is $\gamma(\kappa) > 0$, i.e. perturbations with such wave numbers initiate an instability on the melt surface. The maximum value of the increment follows from expression (6.21): $\gamma_m^2 = (\sigma/\rho)\kappa_m^3$, $\kappa_m = (2/5)^{5/7}\kappa_1$.

The excitation threshold of the EC instability, found from the condition $\gamma = 0$, is

$$I_*(\kappa) = \frac{0.2\kappa\sigma^{5/4}\rho^{-1/4}\kappa^{7/4}}{\varepsilon_T \chi^{1/2}}.$$

For molten steel with $\varepsilon \approx 2 \times 10^3$ dyn cm^{-2}, $\rho = 8$ g cm^{-3}, and $\kappa = 200$ cm^{-1}, numerical estimates give $I_* \approx 5 \times 10^5$ W cm^{-2}. The threshold of deep penetration melting for steel is $I_* \approx 3 \times 10^5$ W cm^{-2} [5]. The maximum increment γ_m is on the order of $\gamma_m \approx 5 \times 10^4$ s^{-1} and the maximum wave number is $\kappa_m \approx 300$ cm^{-1}. Hence, the period of the resultant spatial structure is $d = 2\pi/\kappa_m = 2 \times 10^{-2}$ cm.

If $\varepsilon_T G \kappa^2 \chi^{1/2}/\rho \ll \omega_0^{5/2}$, Eqn (6.20) gives an estimate of the increment $\gamma \approx \mathrm{Re}\left[\varepsilon_T G \kappa^2/2\rho\omega_0(\kappa^2 + \mathrm{i}\omega_0/\chi)^{1/2}\right]$, which is identical with the result given in Ref. [131].

For long wavelengths ($\kappa a \leqslant 1$), when the spatial scale of perturbations is considerably greater than the melt thickness on the walls of a vapour–gas crater and is comparable with the melting depth h, and also if $\varepsilon_T = 0$, the Rayleigh instability [122] follows from Eqn (6.19). In this case the growth of surface perturbations occurs under the influence of the normal component of the surface tension force, resulting from curvature of the walls of the vapour–gas crater. However, the tangential component of the surface tension, associated with the wave corrugation of the free surface, has a stabilising influence. If we assume that the molten layer on the crater walls is sufficiently thin, i.e. $\kappa\delta_k \ll 1$ ($\delta_k = b - a$ is the thickness of the molten layer), the Rayleigh instability increment is described by $\gamma_R^2 = (\sigma/\rho a^2)\kappa^2(1 - \kappa^2 a^2)\delta_k$. Since the minimal wave number $\kappa_{min} = 2\pi/h$, the instability is possible if $h > 2\pi a$. The maximum of the increment is reached at $\kappa = \kappa_m = 0.7a^{-1}$ and it is equal to $\gamma_{Rm} \simeq (\sigma\delta_k\kappa_m^4/\rho)^{1/2}$.

However, if $\varepsilon_T \neq 0$, it follows from Eqn (6.19) with $(\chi\kappa^2/\gamma)^{1/2} \ll 1$ that [148]

$$\gamma^2 \approx \frac{\varepsilon_T G_0 \kappa \delta_k}{\rho a} + \frac{\sigma}{\rho a^2}\kappa^2(1 - \kappa^2 a^2)\delta_k. \tag{6.22}$$

The results of a numerical analysis of Eqn (6.19) are presented in Fig. 3 which gives the dispersion dependences

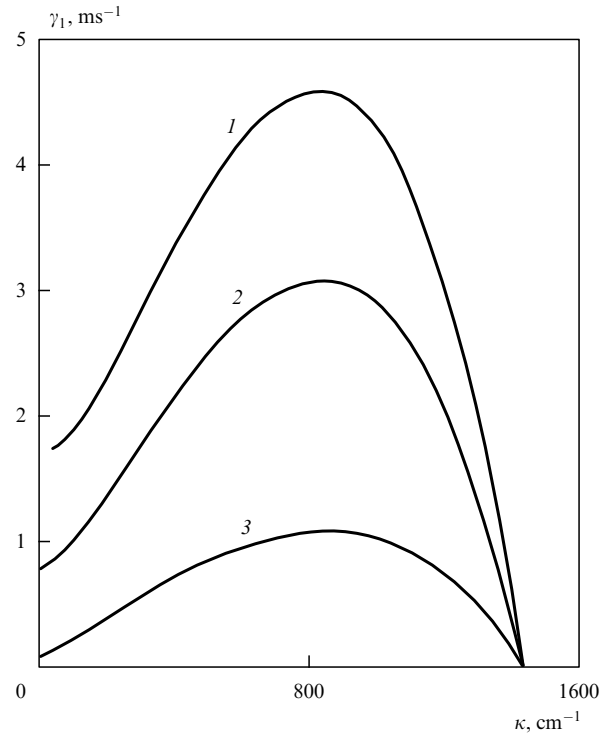

Figure 3. Dispersion dependences for the evaporation–capillary instability, plotted for different values of the parameter s: (*1*) 1.2; (*2*) 1.3; (*3*) 2.0 [147].

of the real part γ_1 of the complex increment $\gamma = \gamma_1 + i\gamma_2$ in that range of the wave numbers where $\gamma_1 > 0$ and the behaviour of hydrodynamic perturbations on the evaporation front is unstable. The linear instability region is bounded from above by $\kappa = 1.4 \times 10^3$ cm^{-1} at $b/a = 1.2$ (curve *1*). Curves *2* and *3* correspond to $b/a = 1.3$ and 2.0, respectively. When the parameter b/a is reduced (or the curvature of the crater walls grows) from 2 to 1.2, the maximal increment γ increases from 658 to 5×10^3 s^{-1}. An increase in the curvature of the crater walls broadens the EC instability region towards long-wavelength perturbations.

We shall now consider azimuthal perturbations [149]. If in Eqn (6.19) we assume that $\kappa \to 0, m \gg 1, \gamma a^2/\chi \gg 1$, the result is

$$\gamma^{5/2} + \omega_0^2 \gamma^{1/2} = \frac{\varepsilon_T G_0 m^2 \chi^{1/2}}{\rho a^3}\,, \tag{6.23}$$

where $\omega_0 = (\sigma m^3/\rho a^3)^{1/2}$.

The solution of Eqn (6.23) for $\varepsilon_T G_0 m^2 \chi^{1/2}/\rho a^3 \gg \omega_0^{5/2}$ reads as [149]:

$$\gamma \approx \frac{\gamma_0^2 - 2\omega_0^2/5}{\gamma_0}\,, \qquad \gamma_0 \approx \left(\frac{\varepsilon_T G_0 m^2 \chi^{1/2}}{\rho a^2}\right)^{2/5}.$$

Hence, the melt surface is unstable if

$$m < m_1 = a^{3/7}\left(\frac{5}{2\sigma}\right)^{5/7} \rho^{1/7} (\varepsilon_T G_0 \chi^{1/2})^{4/7}\,.$$

The maximal increment is reached for

$$m_{\rm m} = a^{3/7} \sigma^{-5/7} \rho^{1/7} (\varepsilon_T G_0 \chi^{1/2})^{4/7}$$

and it is equal to

$$\gamma_{\rm m} = \left(\frac{\varepsilon_T G_0 \chi^{1/2}}{a}\right)^{6/7} (\sigma^2 \rho)^{-2/7}\,.$$

The excitation threshold of the EC instability is

$$I_*(m) = \frac{0.2\varkappa \sigma^{5/4} \rho^{-1/4} (m/a)^{7/4}}{\varepsilon_T \chi^{1/2}}\,.$$

In the other limiting case when $\varepsilon_T G_0 \chi^{1/2} m^2/\rho a^2 \ll \omega_0^{5/2}$, Eqn (6.23) yields

$$\gamma \approx \frac{\varepsilon_T G_0 m^2 \chi^{1/2}}{2\rho a^3 \omega_0^{3/2}}\,.$$

In spite of the fact that the increments of the axisymmetric perturbations are smaller than those of the azimuthal perturbations and that this difference increases with reduction in the thickness of the molten layer on the walls of a crater, both types of perturbation should be observed in the crater. Therefore, under certain conditions this may result in build-up on the melt surface of helical oscillations or waves, whereat the lines of perturbed motion represent helixes moving along their own axes. Solidification of the melt perturbed by such oscillations can account for the observed formation of spiral-like structures on a crystallised melt surface [153].

The limits of validity of the dispersion equation (6.19), when the direct influence of evaporation on modulation of the temperature profile and the velocity of the phase transition front can be ignored, are set by the inequalities $e_1 V_{evT} < q\varkappa$, $G_0 V_{evT}(e_1 l_1 - l_2) < \chi l_0$ [147], which are satisfied well for $V_{evT} G_0 < 25$ cm s^{-1} ($V_{evT} = {\rm d}V_{\rm ev}/{\rm d}T$, where $V_{\rm ev}$ is the evaporation rate).

An increase in the evaporation rate enlarges also its influence on the temperature profile in the melt because of the heat of the phase transition [131]. Moreover, an increase in the vapour recoil pressure magnifies the amplitude of the capillary waves, so that these waves become nonlinear. At amplitudes exceeding $\kappa_{\rm m}^{-1}$ ($\kappa_{\rm m}$ is the maximal wave number) drops may become detached from the crests of capillary waves. As a result, additional flow of molten metal appears across the axis of a crater, in the direction from the front to the rear wall.

In addition to the EC instability, the Rayleigh – Taylor instability (build-up of which occurs during removal of the molten metal by acceleration of the liquid under the action of the vapour recoil pressure) and the capillary–wind instability (due to the influence of near-sonic flow of the vapour along the free surface of a molten metal parallel to the crater axis) may develop.

In general, the structures in a liquid and the structures of a solidified metal can have a variety of forms. These forms depend not only on the energy and spatial – temporal characteristics of laser radiation, but also on the polarisation of this radiation, the angle of tilt relative to the surface, and interference effects. The relationships given above illustrate specific dependences of the parameters of such structures in the melt on the laser radiation characteristics, and a wide range of opportunities for controlling these parameters. However, much is still unclear regarding the influence of these processes on the properties of a solid and of solidified melts. For example, the growth of hydrodynamic instabilities may be accompanied by deterioration of the quality of welds. This is due to nonuniform melting, ejection of the liquid, pores, etc. Hydrodynamic instabilities in a vapour–gas crater may be the reason for the appearance of a one-dimensional lattice of pores along the weld, frequently seen experimentally. However, in spite of the technological importance of this topic, there is no theory as yet and the available experimental data are fragmentary.

6.4 Self-oscillations in the presence of a near-surface plasma

When concentrated energy fluxes $10^5 - 10^7$ W cm^{-2}, constant in time, act on the surface of condensed media, fluctuations of the physical parameters at frequencies $10^2 - 10^4$ Hz are observed in the heated zone [150 – 156]. These fluctuations are the result of the appearance of an oscillatory instability and self-oscillations of the surface temperature of a material and of the density of a weakly ionised low-temperature near-surface plasma. This plasma may be formed from the evaporated material or from the gaseous medium surrounding a metal.

Laser radiation heats the molten surface to the boiling temperature, evaporates some of the material, and heats the vapour until a plasma is formed. The resultant near-surface plasma absorbs strongly the incident laser radiation and defocuses it. As a result, the intensity of the radiation reaching the metal surface falls and so does the melt temperature in the irradiation zone, the vapour of the material is no longer supplied to the plasma, the plasma cloud breaks apart, and the process is repeated, i.e. self-oscillations are observed. The

process has a threshold. The critical energy flux, as well as the amplitude and the frequency of self-oscillations, all depend on the laser beam parameters, on the thermophysical properties of the material, and on the gasdynamic characteristics of the vapour [152].

An analytic description of self-oscillations is provided by a system of equations for the dynamics of the temperature field and the plasma density in a laser jet [154], which lead to time-periodic solutions [155]. This has provided the basis for the analysis of such phenomena as pulsating evaporation, instabilities of evaporation and melting [154], pulsations of the vapour–gas crater [156], and appearance of a periodic relief on the walls of this crater [5].

On the other hand, the very existence of self-oscillations suggests the possibility of a number of new methods for the control of various processes in the irradiation zone. They are associated with, for example, the fact that the temperature field determines the thermophysical processes in a given material (melting, evaporation, hydrodynamic phenomena in the melt, etc.). Moreover, we can use control methods well-tested in nonlinear wave and oscillatory processes, employed already explicitly or implicitly in various technological operations such as, for example, cutting and welding. It is suggested in Ref. [156] that self-oscillations may be suppressed by external modulation which is in antiphase with self-modulation. However, the self-modulation phase is governed by internal nonlinear processes in the irradiation zone, so that it may match the external modulation phase, with the result that the self-oscillations are not suppressed but amplified. Therefore, suppression of self-oscillations requires an additional device which can follow the phase of these oscillations and can ensure that the external modulation is in antiphase.

Self-oscillations may play a significant role in an increase or reduction of the efficiency of the thermal effects of laser radiation on matter. In specific technological operations this is achieved by selecting the optimal pulse repetition frequency. The optimal range of such frequencies is 20 – 60 kHz [156]. In the absence of self-oscillations, the time-dependent component of the intensity has no influence on the average surface temperature. In the presence of self-oscillations, in view of the nonlinear nature of the interaction of laser radiation with these oscillations, the time-dependent term of the energy flux makes a nonzero contribution to the average surface temperature [154]. The magnitude and sign of this contribution depend on the frequency and amplitude of both self-oscillations and the external modulation of the laser radiation intensity. If the relationships between these parameters are selected in such a way that the correction to the average temperature is positive and maximal, it should be possible to increase the efficiency of the thermal effects of laser radiation.

On the whole, it follows from the data on the appearance of various instabilities, accompanied by the excitation of self-waves or self-oscillations in a melt, and from the identification of specific mechanisms that is should be possible to use them for monitoring and control of various thermophysical phenomena in the zone of action of laser radiation on materials.

7. Controlled laser fracture

7.1 Mechanisms of fracture of solids

A new range of phenomena associated with damage processes appears when solids are exposed to laser radiation of $I \geqslant 10^7$ W cm^{-2} intensity. We shall now consider some aspects of the physics of damage, mainly in the case of opaque solids, with the relation to possibility of controlling these processes by means of lasers. Intense irradiation creates a plasma above the surface of a solid and this plasma absorbs laser radiation. Fast heating expands the plasma. The absorbed energy is converted efficiently into a pressure pulse and shock waves propagating in a solid are generated. These shock waves pass through a solid and are reflected from its opposite surface or from inhomogeneities. This may result in splitting of a sample into several parts. All this needs is breaking of bonds along the cleavage surface and not of all the bonds in the bulk, in contrast to melting or evaporation. The difference between the breaking energies needed for fracture and those needed for melting or evaporation differ by a factor of $10^5 - 10^6$. Under real conditions this difference is somewhat less because of the unavoidable losses, such as those associated with — for example — the formation of a plasma or the generation of shock waves and their dissipation.

The process of fracture of a solid by shock waves induced by a laser is determined largely by the microstructure of the solid: the type of lattice, the distribution and interaction of defects, and the presence of stresses. In the case of engineering structures, the fracture and strong deformation may be associated primarily with local energy evolution and shear resulting from the stresses that appear at the points where the elements of such a structure are joined.

The control of fracture processes is closely related to the operational parameters of a laser and the spatial–temporal structure of its radiation. An analysis of opportunities for such control, including the use of a relatively small input energy to cause fracture, should take account of structural relaxation and should be based on the understanding of the mechanisms of the phenomena that occur under the action of laser radiation.

The problem of the strength of solids has a very extensive literature [157 – 159]. According to modern ideas, fracture is regarded as a complex multistage process that depends on a whole range of factors (the nature of a material, the type of stresses, the conditions during service life, the temperature regime, and changes with time). In an ideal case when a body fractures along a certain surface, it is necessary to ensure that the applied force producing a stress σ exceeds the force F binding each pair of atoms separated by the fracture surface. Such a theoretical strength amounts to $\sigma_E \approx 0.1E$, where E is the Young modulus. However, in reality, fracture begins at loads which hundreds and thousands times less than σ_E. This is due to the presence of specific stress concentrators in a solid. The local stresses are particularly high at the edge of a growing crack. For example, in a plate with elliptic hole (crack) of length $2l$ (large axis of ellipse) and the radius R_{el} of curvature close to elongated vertexes, the stress at sharp ends of the hole is $\sigma_{\mathrm{e}} = (1 + 2\sqrt{l/R_{\mathrm{el}}})\sigma_{\mathrm{ex}}$, where σ_{ex} is the stress created by an external force far from the hole. Since the radius of curvature at the tip of a crack is very small and since, in principle, this radius may be regarded as equal to the interatomic distance, it follows from the relationship just given that even a crack 1 μm long can reduce the strength of a

solid by two orders of magnitude. The critical size of a crack, below which it cannot grow spontaneously, was established back in 1920 by Griffith [160]. The critical stress for a crack of this length is

$$\sigma_* \approx \frac{\sqrt{E(\Gamma_s + \Gamma_p)}}{l},$$

where Γ_s is the surface energy and Γ_p is the effective surface energy, which takes account of plastic deformation. When the critical length l_* is reached, an external load is no longer needed to complete the process of fracture: the elastic energy already stored in a solid up to that moment is sufficient. The velocity of propagation of a crack in brittle materials after it reaches the length l_* can rise to values on the order of 10^3 m s^{-1} and the acceleration at this stage of crack growth can be up to 10^8 m s^{-2}. Fracture is always preceded by a greater or smaller degree of plastic deformation. If this deformation is strong not only near the fracture surface, but also in the bulk of a solid, then the fracture is called viscous. It corresponds to the merging of pores and slip.

It is therefore possible to divide a whole process of fracture of solids into three main stages: nucleation of cracks, growth of crack systems to the critical length, and practically instantaneous fracture of a sample. The third stage is uncontrollable, but the first two can be controlled. Two mechanisms of crack nucleation can be distinguished. According to the dislocation mechanism, the application of a stress to a solid creates first elastic and then plastic deformation. Near structural inhomogeneities, which hinder the motion of dislocations, high local stresses and considerable dislocation pile-ups are created and they include those already existing in a sample and those formed by plastic deformation. The interaction of dislocations nucleates microcracks [161]. According to the dilatation mechanism associated with the thermal motion of the lattice atoms under a load, an anharmonic crystal has regions with higher tensile lattice strains, which are called dilatons and which act as nuclei of thermal-fluctuation-induced microcracks. Formation of dilatons and their subsequent opening up to form a microcrack occur near defects [162 – 164].

During the second stage of fracture the newly formed system of microcracks evolves from sizes typically 0.1 – 1 μm to critical values. The concentration of cracks in some parts of a sample may reach 10^{15} cm^{-3}. Above system is then 'conditionally stable', i.e. it is stable against small perturbations but unstable against large ones. Moreover, a crack does not remain unchanged in the presence of stresses: it grows slowly and sometimes this growth is undetectable. A major role in this process is played by the residual stresses resulting largely from heat treatment of some particular engineering structures (for example, near welds). Under abrupt cooling conditions, when plastic deformation ceases to be 'active', embrittlement takes place and critical values of the parameters decrease strongly. As a result, the process may go over to the third uncontrolled stage.

7.2 Dependence of laser induced fracture on the radiation characteristics

We shall now consider specific opportunities for controlling the processes of laser-induced fracture by making use of different lasing regimes. The pressure P generated as a result of a hot plasma cloud expansion under the laser irradiation can be estimated from

$$P = (a_{pl}\tau_p)^{-1/3} I^{3/4}, \tag{7.1}$$

where the coefficient a_{pl} represents the plasma properties and depends on the charge and atomic weight of an ion; τ_p is the pulse duration. For an aluminium target, exposed to laser pulses of $\tau_p = 10^{-8}$ s duration and of $I = 10^{10}$ W cm^{-2} intensity, it follows from expression (7.1) that $P \approx 5 \times 10^{11}$ dyn cm^{-2}. Such laser pulses determine the initial conditions for the propagation of a shock wave. As this wave penetrates a solid, it decays and this process is faster at higher pressures and for shorter pulse durations. During propagation of a shock wave of energy $E_{sh} = (1/2)P(v_0 - v)$ some of this energy is converted irreversibly into heat:

$$Q = \frac{1}{2} P_H(v_0 - v) - \int_v^{v_0} P_s \, dv.$$

Here, v and v_0 are the specific volumes behind and ahead of the shock-wave front. The Hygoniot pressure P_H and the adiabatic pressure P_s are given by phenomenological expressions such as $P_{H,s} = A + B\eta_v^2 + C\eta_v^3$. The values of the constants A, B, C (representing the material) for the pressures P_H and P_s, and the equation for $\eta_v = v_0/v - 1$, as well as its numerical solution can be found in Ref. [165]. Fig. 4 shows the decay of a pressure pulse generated by a laser pulse of $\tau_p = 10^{-7}$ s duration, plotted for different values of η_v. The results of calculations carried out for different values of τ_p show that the shorter the pulse, the lesser the depth to which it penetrates a given material. Hence, we can conclude that there is an opportunity for effective utilisation of a sequence of pulses of increasing duration when the pulses penetrate deeper and deeper into a material.

Shock waves generate stresses in a solid and the existing microcracks begin to expand. In a model [166] of the effect of pulses of duration τ_p and of amplitude σ_0 on cracks of length $2l$, the elastic tensile, kinetic, and surface energies are included, as well as the external work done on a given body. The model is used to drive a differential equation for l and the solution to this equation shows that each pulse, characterised by specific values of the duration and amplitude, selects (from all possible cracks existing in a given sample) a certain range

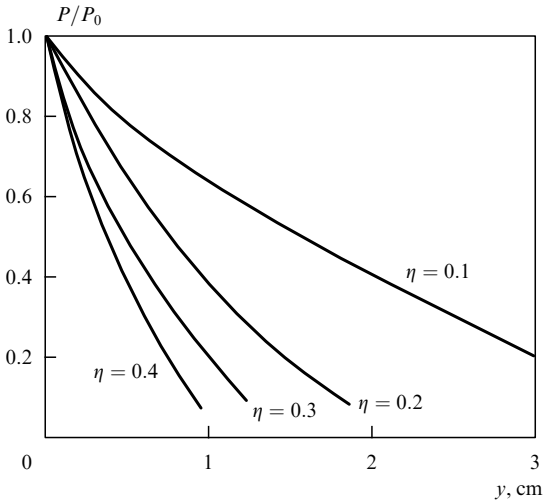

Figure 4. Attenuation of a pressure pulse ($\tau = 10^{-7}$ s) [166].

limited from below and above by the minimal and maximal crack dimensions. Such a pulse acts on cracks which are within this range and these cracks expand. The lower limit of the range is given by [165]

$$l = \frac{\Gamma_s E}{\sigma_0^2} . \tag{7.2}$$

It defines the threshold force necessary for a crack to diverge initially. Pulses of such amplitude may not expand smaller cracks. The upper limit of the range is [165]

$$l = c_{ac}\tau_p , \tag{7.3}$$

where c_{ac} is the velocity of acoustic waves. The physical meaning of formula (7.2) is that, in view of the slowness of the response of a material, a short pulse cannot act on cracks which are too large: it simply does not manage to expand these cracks. Therefore, in contrast to the static case, we have not one but two stability criteria.

Let us consider a specific crack. We assume that it doubles in size under the action of a pulse. This means that the amplitude of the next pulse can be $\sqrt{2}$ times less, but the duration should increase by a factor of 2. If we assume that the pulse energy is $\tau_p\sigma_0^2$, then this energy remains constant. A series of pulses then gradually expands the same group of cracks. The minimum energy of a pulse for a given material is defined by the expression

$$\frac{\sigma_0^2\tau_p}{E} = \frac{\Gamma}{3c_{ac}}$$

which follows directly from formulas (7.2) and (7.3). Therefore, effective fracture of a material may result from the application of a sequence of pulses of decreasing amplitude and increasing duration. The first pulse should be made as short as possible in order to be able to act on the smallest cracks. It should be pointed out that at very high loading rates, associated with high-intensity stress pulses, a material usually regarded as viscous may show brittle behaviour. Additional energy losses due to plastic deformation no longer occur. Therefore, fracture processes can be controlled effectively by selecting a specific time history of laser radiation.

Additional opportunities appear when the spatial structure of laser radiation is utilised. Fracture produced by stress pulses differs from that induced by static forces. In the case of short pulses, only a small part of a sample is in a stressed state and a fracture may occur in one part of a sample, irrespective of what happens elsewhere. If a compression pulse reaches a free boundary, it generates a tension pulse. This may result in, for example, spallation of a part of a material from the opposite side of a plate when the front face is subjected to laser radiation. In the case of oblique reflection, both compression and tension pulses are generated. Interference between such pulses gives rise to complex stress distributions. The result may be the appearance of stresses which are sufficiently high to cause fracture even when the amplitude of the incident pulses is too low for this. Control of fracture by creation of an appropriate spatial structure of laser radiation should take account of the shape of a sample, interference of the reflected waves, as well as attenuation and dissipation of shock waves.

7.3 Role of the solid microstructure in laser fracture

The effects of laser radiation on a solid depend on the specific features of its structure such as dislocations, microcracks, pores, impurities, grain boundaries, stresses, spatial distributions of defects as well as of tension and compression regions. Interaction with a microstructure of a solid may result in an inhomogeneous release of energy and also in change in the characteristics of the propagating wave. Much depends on the characteristics of the radiation itself. It is illuminating to consider the effects of laser radiation on transparent materials such as polymers, glasses, etc. The problem of laser damage to transparent solids is on the whole more complex than the corresponding problem in the case of opaque solids, and the fracture mechanisms (particularly at the initiation stage) are very different [166, 167]. The dependence of the fracture on the laser operation regime is particularly strong in the case of transparent materials. It is found that the ability of ordinary polymeric materials to withstand high-power laser radiation under the action of repeated pulses is considerably less than for a single pulse [168]. Manenkov et al. [169–172], who investigated the relationships governing the process of fractural transparent polymers, have established the existence of a cumulative effect in the case of repeated laser irradiation. The process begins with energy evolution at absorbing defects and can be divided into two stages: slow and fast. The first (slow) stage results in evolution of an absorbing defect between the pulses: this happens at a velocity $< 10^3$ cm s^{-1} and produces microdamage up to 1 μm in size. During the fast stage, a crack appears in a threshold manner and its dimensions are in excess of 1 μm, which increases at a considerable velocity ($\geqslant 10^4$ cm s^{-1}) up to 10–30 μm as a result of interaction with subsequent pulses, until a crack of about 100 μm size is formed. In contrast to the first stage, this stage is accompanied by the emission of considerable radiation in the visible and near-ultraviolet regions. The temperature is estimated to be 10^4 K and the duration of such radiation pulses is 10^{-7} s. During the second stage the fracture process involves the appearance of an ionisation–absorption wave at each pulse [173].

When a single pulse is applied to a solid, its intensity I_1 is governed by the possibility of appearance of an ionisation wave. The process of multiple fracture may occur at relatively low laser radiation intensities ($I \ll I_1$). A mechanism for the first stage of the process of laser fracture was proposed in Refs [170, 172]. When laser pulses act on a polymer, the absorption of the laser radiation energy by various defects and inclusions generates elastic stresses in the surrounding host material and these stresses are comparable with the breaking strength of polymers. Such pulsed stresses result, in combination with residual static stresses, in mechanical damage to the polymer host material and consequent formation of vibrationally excited radicals which absorb laser radiation. Experiments show [172] that the concentration of radicals can be very high, reaching 10^{21} cm^{-3}.

Residual stresses accumulate around inclusions during the action of the subsequent laser pulses. As a result, the rate of formation of excited radicals increases and this enhances the absorption of the incident radiation. When a certain critical value is exceeded, the stability is lost, an absorption wave propagates, and microfracture occurs. Just this critical value is the threshold for multipulse fracture. During subsequent irradiation the microcrack dimensions gradually increase up to macroscopic sizes.

A similar, although less pronounced, is the cumulative effect in glasses [174–176]. It depends strongly on the conditions during irradiation (pulse repetition frequency) and on the microstructure of samples. Once again, the process begins from structural changes which appear at absorbing microinhomogeneities [174].

In the processes of laser damage the cumulative effect is accompanied also by a dimensional dependence, i.e. a dependence on the size of the irradiated region [177–179]. The presence of a high concentration of defects which have a significant influence on the strength has the effect that high damage thresholds ($10^{10}-10^{11}$ W cm^{-2}) are observed only for very tiny regions ($10^{-8}-10^{-10}$ cm^3). When the irradiated region is increased, the damage threshold falls because of an enhancement in the probability that the defects influencing this threshold will be found in the region. Moreover, mutual influence of two spatially separated focused laser beams has been found. In this case the damage threshold depends on the distance between the beams [179]. A spatially inhomogeneous structure of laser pulses is more favourable for damage. Therefore, damage to transparent solids can be controlled effectively by selecting some specific spatial–temporal structure of laser radiation.

In the case of opaque solids a considerable influence on the damage process is exerted by the interaction between shock waves, initiated by laser radiation, and defects. The possibility of spatial focusing of a shock wave and a change in its temporal structure by a system of pores has been considered. Heating and the resultant increase in the plasticity of a metal may give rise to cavitation phenomena. The pores are then compressed and collapsed releasing large amounts of energy. Cumulative thin streams may form and they can cause additional damage to a solid. Formation of such thin streams is particularly effective in the case of cylindrical, conical, and some other shapes of cavities [180].

Vulnerable parts of engineering structures subjected to laser radiation are the points where elements of a structure are joined, where stretched regions, residual stresses, and high defect concentrations can be found. Enhanced local energy dissipation occurs in these regions under the action of laser–excited shock waves and additional stresses are created. Equally, in the case of transparent solids, the cumulative effect is active in such regions and relatively weak multipulse irradiation can bring an engineering structure close to its stability limit.

8. On cybernetic aspects of laser control

We have to consider, even if briefly, the cybernetic aspects of the problem. As pointed out already, a laser beam with its energy, spectral, spatial, and temporal characteristics can be used for effective control of a very great variety of the processes that occur in a solid, ranging from crystal growth to fracture. For a large number of processes, it is possible to select a specific laser 'key' which makes it possible to act selectively on these processes and to create numerous complex structures. Different parameters of irradiation of a solid and self-organisation effects may give rise to succession of various forms of a solid. The succession is characterised by a complex system of mutual dependences, nonlinear interactions, feedback, and instabilities, which carry together an enormous amount of information.

Any form of control is closely related to the effects of information. A special feature of a laser beam is that it can carry a large amount of information necessary for the activation of some specific processes. Each element of a structure and each defect subsystem has its own features, its own channels for action, and its own risk factors. Understanding of these features opens up definite possibilities of the formation of structures with given properties. We can therefore speak of the beginning of a new generation of laser technologies based on the selection of specific 'keys' for the various processes that occur in a solid and can be used to control these processes.

From the cybernetic point of view, effective control requires information on the states of the system and on how these states change. In addition to identifying the relationships of the processes that occur, control procedures may utilise information on the current state of an object obtained by a variety of detectors and sensors. An important step in this direction has been made in the eighties: laser systems utilising feedback have become available. An example is the equipment made by Vanzetti Systems [181] for soldering and monitoring of joints, which is used in the manufacture of integrated circuits and in which a suitably programmed detector is employed. An infrared signal emitted in the course of laser welding reaches this detector and the detector output signal is converted to a digital form. A computer then compared the characteristics of the resultant signal with those from a standard sample. A laser beam is interrupted by a signal from a computer at the moment when the solder begins to flow, or when a defective joint is formed, and also when a beam becomes misaligned. Equipment of this type is sometimes called 'intelligent'.

Widening the range of applications for such equipment requires the development and improvement of detectors. For example, in addition to infrared detectors, it would be desirable to use a detector of acoustic signals excited by a laser and carrying information about the processes occurring in the irradiation zone [182]. A detector would follow the processes in a solid and the equipment would control the duration (and other properties) of laser radiation, so as to alter the effects of such radiation in the desired direction for obtaining a specified result.

One can speak here of some biological analogies. Characteristic terms have parallels with those describing a living organism: fatigue and survival of a material, shape memory, sickness of a metal, corrosion stability, etc. This is not a purely formal similarity: it reflects the reality of the phenomena.

The kinetics of the processes that occur in a solid occupies a kind of intermediate position between the kinetics of the processes that occur in biology [183] and in gases [18]. Stability is typical in the theory of gases and of classical physics as a whole. In biology, stability is an exception rather than the rule. Evolution is an infinite chain of replacement of one stable state by another, passing through instabilities. Any living system (organism, population, biocenosis) survives only a finite time. It is stable only during that time.

The situation is very similar also in the case of structures in a solid which is exposed to laser radiation. In a living organism there is a complex interplay of chemical reaction cascades in which the product of one reaction becomes the starting material for another. Similarly, in a solid, there are chains of dissipative structures and each of them is the starting point for those that follow it. However, on the whole, the processes of self-organisation in a solid in the presence of feedback, maintained by sensors and a computer

with a control device, offer a hope that it should be possible to construct systems which include lasers, solids, and computers and which are in many ways similar to biological systems and are capable of continuous evolution.

Acknowledgements. We are grateful to V S Golubev, V I Emel'yanov, G A Kalyuzhnaya, T S Mamedov, and V N Seminogov for stimulating discussions. The authors are grateful to the International Science Foundation (Grant No. NLH300), the Russian Fund for Fundamental Research, and also INTAS-94-0902 for financial support.

References

1. Anisimov S I et al. *Deistvie Izlucheniya Bol'shoi Moshchnosti na Metally* (Effects of High-Power Radiation on Metals) (Moscow: Nauka, 1970)
2. Ready J F *Industrial Applications of Lasers* (New York: Academic Press, 1978)
3. Vedenov A A, Gladush G G *Fizicheskie Protsessy pri Lazernoi Obrabotke Materialov* (Physical Processes in Laser Treatment of Materials) (Moscow: Énergoatomizdat, 1985)
4. Duley W W *Laser Processing and Analysis of Materials* (New York: Plenum Press, 1983)
5. Arutyunyan R V et al. *Vozdeistvie Lazernogo Izlucheniya na Materialy* (Effects of Laser Radiation on Materials) (Moscow: Nauka, 1989)
6. Rykalin N N et al. *Lazernaya i Électronno-Luchevaya Obrabotka Materialov* (Laser and Electron-Beam Processing of Materials) (Moscow: Mashinostroenie, 1985)
7. Abil'siitov G A et al. *Moshchnye Gazorazryadnye CO_2-Lazery i ikh Primeneniya v Technologii* (High-Power Gas-Discharge CO_2 Lasers and Their Applications in Technology) (Moscow: Nauka, 1984)
8. Dvurechenskiĭ A V et al. *Impuls'snyi Otzhig Poluprovodnikovykh Materialov* (Pulsed Annealing of Semiconductor Materials) (Moscow: Nauka, 1982)
9. Panchenko V Ya, Seminogov V N, Khudobenko A I *Kvantovaya Elektron.* (*Moscow*) **16** 1226 (1989) [*Sov. J. Quantum Electron.* **19** 794 (1989)]
10. Weaver L A "Machining and Welding Applications", in *Laser Applications* (Ed. M Ross) Vol. 1 (New York: Academic Press, 1971) p. 270
11. Houle F A *Appl. Phys. A* **41** 315 (1986)
12. Levinson G R, Smilga V I *Kvantovaya Elektron.* (*Moscow*) **3** 1637 (1976) [*Sov. J. Quantum Electron.* **6** 885 (1976)]
13. Artamonova N D, Platonenko V T, Khokhlov R V *Zh. Eksp. Teor. Fiz.* **58** 2195 (1970) [*Sov. Phys. JETP* **31** 1185 (1970)]
14. Krasnov I V, Shaparev N Ya, Shkedov I M *Optimal' nye Lazernye Vozdeistviya* (Optimal Laser Effects) (Novosibirsk: Nauka, 1989)
15. Panchenko V Ya, Tolstoshein A A *Khim. Fiz.* **6** 16 (1987)
16. Panchenko V Ya et al. A I *Izv. Ross. Akad. Nauk Ser. Fiz.* **36** 91 (1992)
17. Panchenko V Ya, Seminogov V N, Sokolov V I *Itogi Nauki Tekh.* **3** 91 (1989)
18. Gordiets B F, Osipov A I, Shelepin L A *Kineticheskie Protsessy v Gazakh i Molekulyarnye Lazery* (Kinetic Processes in Gases and Molecular Lasers) (Moscow: Nauka, 1980)
19. *Lasers Optronics* **7** 55 (1988)
20. *Electronics* **60** 34 (1987)
21. Gordiets B F, Osipov A I, Panchenko V Ya *Tr. Fiz. Inst. Akad. Nauk SSSR* **107** 68 (1979)
22. Medvedev S A, Ivannikova G E *Elektron. Tekh. Poluprovodn. Prib.* **4** 29 (1970)
23. Guro G M et al. *Tr. Fiz. Inst. Akad. Nauk SSSR* **124** 127 (1980)
24. Guro G M et al. *Zh. Eksp. Teor. Fiz.* **77** 2366 (1979) [*Sov. Phys. JETP* **50** 1141 (1979)]
25. Guro G M et al. *Tr. Fiz. Inst. Akad. Nauk SSSR* **177** 85 (1987)
26. Kalyuzhnaya G A, Kiseleva K V *Tr. Fiz. Inst. Akad. Nauk SSSR* **177** 5 (1987)
27. Burton W K, Cabrera N, Frank F C *Philos. Trans. A* **243** (866) 299 (1951)
28. Baru V G, Vol'kenshteĭn F F *Vliyanie Oblucheniya na Poverkhnostnye Svoistva Poluprovodnikov* (Influence of Irradiation on Surface Properties of Semiconductors) (Moscow: Nauka, 1978)
29. Bol'shova K V, Levchenko I S, Shubin A A *Prib. Tekh. Eksp.* (2) 228 (1968)
30. Geguzin Ya E *Diffuzionnaya Zona* (Diffusion Zone) (Moscow: Nauka, 1979)
31. Gorina Yu I et al. *Fiz. Tekh. Poluprovodn.* **13** 305 (1975) [*Sov. Phys. Semicond.* **13** 175 (1979)]
32. Osip'yan Yu A, Savchenko I B *Pis'ma Zh. Eksp. Teor. Fiz.* **7** (4) 130 (1968) [*JETP Lett.* **7** (4) 100 (1968)]
33. Osip'yan Yu A, Petrenko V F, Savchenko I B *Pis'ma Zh. Eksp. Teor. Fiz.* **13** (11) 622 (1971) [*JETP Lett.* **13** (11) 442 (1971)]
34. Osip'yan Yu A, Petrenko V F, Shikhsaidov M Sh *Pis'ma Zh. Eksp. Teor. Fiz.* **20** 363 (1974) [*JETP Lett.* **20** (6) 163 (1974)]
35. Osip'yan Yu A, Petrenko V F *Pis'ma Zh. Eksp. Teor. Fiz.* **17** (10) 555 (1973) [*JETP Lett.* **17** (10) 399 (1973)]
36. Aleksandrov O V et al. *Kratk. Soobshch. Fiz.* (2) 45 (1984)
37. Bauerle D *Europhys. News* **14** 9 (1983)
38. Zaĭtsev V V et al. *Zh. Tekh. Fiz.* **55** 955 (1985) [*Sov. Phys. Tech. Phys.* **30** 573 (1985)]
39. Mamedov T S et al. *Kvantovaya Elektron.* (*Moscow*) **20** 714 (1993) [*Quantum Electron.* **23** 620 (1993)]
40. Arzuov M I et al. *Pis'ma Zh. Tekh. Fiz.* **5** 193 (1979) [*Sov. Tech. Phys. Lett.* **5** 76 (1979)]
41. Prokhorov A M et al. *Vzaimodeistvie Lazernogo Izlucheniya s Metallami* (Interaction of Laser Radiation with Metals) (Moscow: Nauka, 1988)
42. Wautelet M *Appl. Phys. A* **50** 131 (1990)
43. Schafer S A, Lyon S A *Philos. Mag. B* **55** 261 (1987)
44. Burmistrov A I, Konov V I *Fiz. Khim. Obrab. Mater.* (3) 3 (1982)
45. Aleksandrov L N *Kinetika Kristallizatsii i Perekristallizatsii Poluprovodnikovykh Plenok* (Kinetics of Crystallisation and Recrystallisation of Semiconductor Films) (Novosibirsk: Nauka, 1985)
46. Ready J F *Proc. IEEE* **70** 533 (1982)
47. Van Vechten J A et al. *Phys. Lett. A* **74** 417 (1979)
48. Boyd I W *Contemp. Phys.* **24** 461 (1983)
49. Boyd I W *Appl. Phys. Lett.* **42** 728 (1983)
50. Blum S E, Brown K H, Srinivasan R *Appl. Phys. Lett.* **43** 1026 (1983)
51. Eggermont Y E, Falster R, Hahn S K *Solid State Technol.* **26** 171 (1983)
52. Bobyrev V A et al. *Izv. Akad. Nauk SSSR Ser. Fiz.* **51** 1180 (1987) [*Bull. Acad. Sci. USSR Ser. Phys.* **51** (6) 130 (1987)]
53. Kelly A, Groves G W *Crystallography and Crystal Defects* (London: Longmans, 1970)
54. Markevich M I, Chaplanov A M *Metallofizika* (*Kiev*) **7** 100 (1985)
55. Boĭko V I, Luk'yanchuk B S, Tsarev E R *Tr. Inst. Obshch. Fiz. Akad. Nauk* **30** 6 (1991)
56. Veĭko V P et al. *Izv. Akad. Nauk SSSR Ser. Fiz.* **49** 1236 (1985)
57. Bychkov Yu A, Mirzoev F Kh, Panchenko V Ya *Proc. SPIE Int. Soc. Opt. Eng.* **1352** 140 (1990)
58. Kornyushin Yu V *Yavleniya Perenosa v Real'nykh Kristallakh vo Vneshnikh Polyakh* (Transport Phenomena in Real Crystals Subjected to External Fields) (Kiev: Naukova Dumka, 1985)
59. Gorobeĭ N N *Fiz. Tverd. Tela* (*Leningrad*) **28** 2252 (1986) [*Sov. Phys. Solid State* **28** 1264 (1986)]
60. Emel'yanov V I, Mirzoev F Kh, Shelepin L A *Kvantovaya Elektron.* (*Moscow*) **24** 769 (1994) [*Quantum Electron.* **24** 714 (1994)]
61. Haken H *Introduction to Synergetics: Nonequilibrium Phase Transition and Self-Organization in Physics, Chemistry, and Biology* 3rd edition (Berlin: Springer, 1983)
62. Nicolis G, Prigogine I R *Self-Organisation in Non-Equilibrium Systems: From Dissipative Structures to Order Through Fluctuations* (New York: Wiley, 1977)
63. Asmus J F, Baker F S *Record of the Tenth Symposium on Electron, Ion, and Laser Beam Technology, Gaithersburg, MD, 1969,* p. 241
64. Veĭko V P et al. *Dokl. Akad. Nauk SSSR* **208** 587 (1973) [*Sov. Phys. Dokl.* **18** 83 (1973)]
65. Karlov N V, Kirichenko N A, Luk'yanchuk B S *Lazernaya Termokhimiya* (Laser Thermochemistry) (Moscow: Nauka, 1992)
66. Bobyrev V A et al. *Poverkhnost'* (4) 134 (1984)
67. Bobyrev V A et al. *Kvantovaya Electron.* (*Moscow*) **10** 793 (1983)

68. Bunkin F V, Kirichenko N A, Luk'yanchuk B S *Usp. Fiz. Nauk* **138** 45 (1982) [*Sov. Phys. Usp.* **25** 662 (1982)]
69. Buzykin O G, Burmistrov A V *Poverkhnost'* (12) 63 (1982)
70. Anisimov N R *Pis'ma Zh. Tekh. Fiz.* **8** 1320 (1982) [*Sov. Tech. Phys. Lett.* **8** 569 (1982)]
71. Gol'berg S M, Tribel'skiĭ M I *Pis'ma Zh. Tekh. Fiz.* **8** 178 (1982) [*Sov. Tech. Phys. Lett.* **8** 77 (1982)]
72. Alimov D T et al. *Poverkhnost'* (9) 82 (1982)
73. Alimov D T, Atabaev Sh, Bunkin F V *Poverkhnost'* (8) 12 (1982)
74. Langer J S *Rev. Mod. Phys.* **52** 1 (1980)
75. Bobyrev V A et al. *Kvantovaya Elektron.* (*Moscow*) **9** 1943 (1982) [*Sov. J. Quantum Electron.* **12** 1267 (1982)]
76. Kalandarishvili K G, Koval'chuk Yu V, Portnoĭ E L *Pis'ma Zh. Tekh. Fiz.* **8** 436 (1982) [*Sov. Tech. Phys. Lett.* **8** 191 (1982)]
77. Bagratashvili V N et al. Preprint No. 32 (Troitsk: Scientific-Research Institute of Industrial Lasers, USSR Academy of Sciences, 1987)
78. Rothschild M, Arnone C, Ehrlich D J *J. Mater. Res.* **2** 244 (1987)
79. Mogyorosi P, Piglmayer K, Bauerle D *Surf. Sci.* **208** 232 (1989); Bauerle D *Appl. Phys. A* **48** (6) 527 (1989)
80. Eshelby J D *Solid State Phys.* **3** 79 (1956)
81. Kosevich A M *Fizicheskaya Mekhanika Real'nykh Kristallov* (Physical Mechanics of Real Crystals) (Kiev: Naukova Dumka, 1981)
82. De Diego N, Kirn M, Ruhle M *Acta Metall.* **27** 1445 (1979)
83. Horz G, Popovic M *Acta Metall.* **27** 1453 (1979)
84. Sidorenko F A, Él'ner V Ya, Gel'd P V *Fiz. Tverd. Tela* (*Leningrad*) **22** 619 (1980) [*Sov. Phys. Solid State* **22** 364 (1980)]
85. Sugakov V I, Preprint No. 70P (Kiev: Institute of Theoretical Physics, Academy of Sciences of the Ukrainian SSR, Kiev, 1984)
86. Evans J H *Nature* (*London*) **229** (5284) 403 (1971)
87. Veĭko V P et al. *Izv. Akad. Nauk SSSR Ser. Fiz.* **49** 1236 (1985) [*Bull. Acad. Sci. USSR Ser. Phys.* **49** (6) 186 (1985)]
88. Budzulyak I M et al. *Izv. Akad. Nauk SSSR Ser. Fiz.* **49** 765 (1985) [*Bull. Acad. Sci. USSR Ser. Phys.* **49** (4) 127 (1985)]
89. Emel'yanov V I et al. *Fiz. Tverd. Tela* (*Leningrad*) **30** 2259 (1988) [*Sov. Phys. Solid State* **30** 1304 (1988)]
90. Bugaev A A, Kolochkov A V *Fiz. Tverd. Tela* (*Leningrad*) **26** 3487 (1984) [*Sov. Phys. Solid State* **26** 2100 (1984)]
91. Verner I V, Tsukanov V V *Zh. Tekh. Fiz.* **55** 2236 (1985) [*Sov. Phys. Tech. Phys.* **30** 1322 (1985)]
92. Devyatko Yu N, Tronin V N *Pis'ma Zh. Eksp. Teor. Fiz.* **37** 278 (1983) [*JETP Lett.* **37** 330 (1983)]
93. Vasilevskiĭ M I, Ershov S N, Panteleev V A *Fiz. Tverd. Tela* (*Leningrad*) **27** 2282 (1985) [*Sov. Phys. Solid State* **27** 1369 (1985)]
94. Emel'yanov V I, Preprint No. 5 (Moscow: Physics Department, Moscow State University, 1985)
95. Emel'yanov V I *Tez. Dokl. IV Mezhd. Simp. po Prob. St. Mekh., Dubna, 1988* (Abstracts of Papers presented at Fourth International Symposium on Problems in Statistical Mechanics, Dubna, 1988) (Dubna: Joint Institute for Nuclear Research, 1988) p. 119
96. Emel'yanov V I, Uvarova I F *Zh. Eksp. Teor. Fiz.* **94** (8) 255 (1988) [*Sov. Phys. JETP* **67** 1662 (1988)]
97. Emel'yanov V I, Uvarova I F *Metallofizika* (*Kiev*) **11** (5) 101 (1989)
98. Emel'yanov V I, Uvarova I F *Fiz. Khim. Obrab. Mater.* (2) 12 (1990)
99. Mirzoev F Kh, Panchenko V Ya, Shelepin L A, Preprint No. 88 (Moscow: Lebedev Physics Institute, Academy of Sciences of the USSR, 1989)
100. Mirzoev F Kh, Panchenko V Ya, Shelepin L A *J. Sov. Laser Res.* **10** 404 (1989)
101. Alieva M A, Mirzoev F Kh, Shelepin L A *Kratk. Soobshch. Fiz.* (3) 9 (1990)
102. Emel'yanov V I, Sumbatov A A *Poverkhnost'* (7) 122 (1988)
103. Emel'yanov V I *Laser Phys.* **2** 390 (1992)
104. Banishev A F et al. *Fiz. Tverd. Tela* (*Leningrad*) **32** 2529 (1990) [*Sov. Phys. Solid State* **32** 1469 (1990)]
105. Mirzoev F Kh, Shelepin L A *Pis'ma Zh. Tekh. Fiz.* **17** (5) 31 (1991) [*Sov. Tech. Phys. Lett.* **17** 168 (1991)]
106. Alieva M A et al. *Kratk. Soobshch. Fiz.* (10) 43 (1988) [*Sov. Phys. Lebedev Inst. Rep.* (10) 60 (1988)]
107. Landau L D et al. *Theory of Elasticity* 3rd edition (Oxford: Pergamon Press, 1986)
108. Sugakov V I *Fiz. Tverd. Tela* (*Leningrad*) **28** 2441 (1986) [*Sov. Phys. Solid State* **28** 1336 (1986)]; Golineĭ I Yu, Sugakov V I *Metallofizika* (*Kiev*) **7** (2) 108 (1985)
109. Kerner B S, Osipov V V *Mikroelektronika* (*Akad. Nauk SSSR*) **12** 502 (1983)
110. Kerner B S, Osipov V V *Usp. Fiz. Nauk* **160** (9) 1 (1990) [*Sov. Phys. Usp.* **33** 679 (1990)]
111. Selishchev P A, Sugakov V I *Fiz. Tverd. Tela* (*Leningrad*) **30** 2611 (1988) [*Sov. Phys. Solid State* **30** 1503 (1988)]
112. Selishchev P P, Sugakov V I *Metallofizika* (*Kiev*) **12** 106 (1990)
113. Mirzoev F Kh, Fetisov E P, Shelepin L A *Tr. Fiz. Inst. Akad. Nauk SSSR* **177** 99 (1987)
114. Volodin B L, Emel'yanov V I *Kvantovaya Elektron.* (*Moscow*) **17** 648 (1990) [*Sov. J. Quantum Electron.* **20** 574 (1990)]
115. Davydov A S *Teoriya Tverdogo Tela* (Solid-State Theory) (Moscow: Nauka, 1986)
116. Palatnik L S, Cheremskoĭ P G, Fuks M Ya *Pory v Plenkakh* (Pores in Films) (Moscow: Énergoizdat, 1982)
117. Kryuchenko Yu V, Sugakov V I *Phys. Status Solidi B* **111** 177 (1982)
118. Rudko V N, Sugakov V I *Phys. Status Solidi B* **126** 703 (1984)
119. Akhiezer I A, Davydov L N, Spol'nik Z A *Fiz. Met. Metalloved.* **43** 937 (1977)
120. Mirzoev F Kh, Fetisov E P, Shelepin L A *Pis'ma Zh. Tekh. Fiz.* **17** 31 (1991) [*Sov. Tech. Phys. Lett.* **17** 168 (1991)]
121. Mirzoev F Kh et al., Preprint No. 17 (Moscow: Engineering–Physics Institute, 1986)
122. Mirzoev F Kh, Fetisov E P, Shelepin L A *Tr. Fiz. Inst. Akad. Nauk SSSR* **177** 121 (1987)
123. Mirzoev F Kh, Fetisov E P, Shelepin L A *Kratk. Soobshch. Fiz.* (6) 30 (1986)
124. Landau L D, Lifshitz E M, Pitaevskiĭ L P *Fluid Mechanics* 2nd edition (Oxford: Pergamon Press, 1987)
125. Maksimov L A, Ryazanov A I *Zh. Eksp. Teor. Fiz.* **79** 2311 (1980) [*Sov. Phys. JETP* **52** 1170 (1980)]
126. Demchuk A V, Danilovich N J, Labunov V A *Poverkhnost'* (11) 26 (1985)
127. Uglov A A et al. *Modelirovanie Teplofizicheskikh Protsessov Impul'snogo Lazernogo Vozdeistviya na Metally* (Simulation of Thermophysical Processes in Pulsed Laser Action on Metals) (Moscow: Nauka, 1991)
128. Locke E V, Hoag E D, Hella R A *IEEE J. Quantum Electron.* **QE-8** 132 (1972)
129. Akhmanov S A et al. *Usp. Fiz. Nauk* **147** 675 (1985) [*Sov. Phys. Usp.* **28** 1084 (1985)]
130. Emel'yanov V I, Seminogov V N *Itogi Nauki Tekh.* **1** 118 (1988)
131. Samokhin A A *Tr. Inst. Obshch. Fiz. Akad. Nauk* **13** 2 (1988)
132. Birnbaum M *J. Appl. Phys.* **36** 3688 (1965)
133. Anisimov V N et al. *Poverkhnost'* (7) 138 (1983)
134. Jain A K et al. *J. Appl. Phys.* **52** 4882 (1981)
135. Keilmann F *Phys. Rev. Lett.* **51** 2097 (1983)
136. Konov V I et al. *Poverkhnost'* (1) 128 (1985)
137. Emel'yanov V I et al., Preprint No. 89 (Moscow: Institute of General Physics, Academy of Sciences of the USSR, 1987)
138. Keilmann F, Bai Y H *Appl. Phys. A* **29** 9 (1982)
139. Arata Y, Abe N, Oda T *Proceedings of Fifth International Symposium on Materials Processing (International Conference on Applications of Lasers and Electro-Optic Technology) Boston, Ma, 1984* p. 72
140. Hutley M C, Maystre D *Opt. Commun.* **19** 431 (1976)
141. Ursu I et al. *Appl. Phys. Lett.* **45** 365 (1984)
142. Arutyunyan R V, Bol'shov L A *Poverkhnost'* (11) 5 (1985)
143. Bugaev A A et al. *Pis'ma Zh. Tekh. Fiz.* **12** 220 (1986) [*Sov. Tech. Phys. Lett.* **12** (2) 91 (1986)]; *Fiz. Tverd. Tela* (*Leningrad*) **28** 1484 (1986) [*Sov. Phys. Solid State* **28** 836 (1986)]
144. Levchenko E B, Chernyakov A L *Zh. Eksp. Teor. Fiz.* **81** 202 (1981) [*Sov. Phys. JETP* **54** 102 (1981)]
145. Ledenev V I, Mirzoev F Kh *Kvantovaya Elektron.* (*Moscow*) **20** 1185 (1993) [*Quantum Electron.* **23** 1030 (1993)]
146. Bunkin F V, Tribel'skiĭ M I *Usp. Fiz. Nauk* **130** 193 (1980) [*Sov. Phys. Usp.* **23** 105 (1980)]
147. Mirzoev F Kh, Shelepin L A *J. Sov. Laser Res.* **16** 3 (1994)
148. Mirzoev F Kh *Kvantovaya Elektron.* (*Moscow*) **21** 147 (1994) [*Quantum Electron.* **24** 138 (1994)]
149. Mirzoev F Kh *Poverkhnost'* (10) 32 (1994)

150. Postacioglu N, Kapadia P, Dowden J *J. Phys. D* **22** 1050 (1989)
151. Bukatyĭ V I, Pogodaev V A, Chaporov D P *Zh. Prikl. Mekh. Tekh. Fiz.* **20** 30 (1979) [*J. Appl. Mech. Tech. Phys.* **20** 22 (1979)]
152. Rykalin N N et al. *Zh. Eksp. Teor. Fiz.* **85** 1953 (1983) [*Sov. Phys. JETP* **58** 1134 (1983)]
153. Banishev A F et al. *Izv. Ross. Akad. Nauk Ser. Fiz.* **57** (12) 99 (1993) [*Bull. Russ. Acad. Sci. Ser. Phys.* **57** 2146 (1993)]
154. Uglov A A, Selishchev S V *Avtokolebatel'nye Protsessy pri Vozdeistvii Kontsentrirovannykh Potokov Energii* (Self-Oscillatory Processes Under the Action of Concentrated Energy Fluxes) (Moscow: Nauka, 1987)
155. Landa P S *Avtokolebaniya v Sistemakh s Konechnym Chislom Stepenei Svobody* (Self-Oscillations in Systems with a Finite Number of Degrees of Freedom) (Moscow: Nauka, 1980)
156. Uglov A A, Selishchev S V *Itogi Nauki Tekh.* **20** 61 (1989)
157. Regel' V R, Slutsker A I, Tomashevskiĭ É E *Kineticheskaya Priroda Prochnosti Tverdykh Tel* (Kinetic Nature of the Strength of Solids) (Moscow: Nauka, 1974)
158. *Mekhanika Razrusheniya. Razrushenie Materialov* (Mechanics of Fracture. Fracture of Materials) (Moscow: Nauka, 1979)
159. Rabotnov Yu N *Vvedenie v Mekhaniku Razrusheniya* (Introduction to Mechanics of Fracture) (Moscow: Nauka, 1987)
160. Griffith A A *Philos. Trans. R. Soc. London Ser. A* **221** 163 (1920)
161. Vladimirov V I *Fizicheskaya Priroda Razrusheniya Metallov* (Physical Nature of Fracture of Metals) (Moscow: Metallurgiya, 1984)
162. Kusov A A *Fiz. Tverd. Tela* (*Leningrad*) **21** 3095 (1979) [*Sov. Phys. Solid State* **21** 1781 (1979)]
163. Zhurkov S N *Fiz. Tverd. Tela* (*Leningrad*) **25** 3119 (1983) [*Sov. Phys. Solid State* **25** 1797 (1983)]
164. Petrov V A *Fiz. Tverd. Tela* (*Leningrad*) **25** 3110 (1983) [*Sov. Phys. Solid State* **25** 1800 (1983)]
165. Steverding B, Dudel H P *J. Appl. Phys.* **47** 1940 (1976)
166. Manenkov A A, Prokhorov A M *Usp. Fiz. Nauk* **148** 179 (1986) [*Sov. Phys. Usp.* **29** 104 (1986)]
167. Dyumaev K M et al. *Tr. Inst. Obshch. Fiz. Akad. Nauk* **33** 3 (1991)
168. Ashkinadze B M et al. *Zh. Eksp. Teor. Fiz.* **50** 1187 (1966) [*Sov. Phys. JETP* **23** 788 (1966)]
169. Manenkov A A, Nechitaĭlo V S *Kvantovaya Elektron.* (*Moscow*) **7** 616 (1980) [*Sov. J. Quantum Electron.* **10** 347 (1980)]
170. Dyumaev K M et al. *Kvantovaya Elektron.* (*Moscow*) **10** 810 (1983) [*Sov. J. Quantum Electron.* **13** 503 (1983)]; *Izv. Akad. Nauk SSSR Ser. Fiz.* **49** 1084 (1985) [*Bull. Acad. Sci. USSR Ser. Phys.* **49** (6) 42 (1985)]
171. Manenkov A A et al. *Kvantovaya Elektron.* (*Moscow*) **11** 839 (1984) [*Sov. J. Quantum Electron.* **14** 568 (1984)]
172. Timashev S F *Dokl. Akad. Nauk SSSR* **276** 898 (1984)
173. Manenkov A A et al. *Kvantovaya Elektron.* (*Moscow*) **10** 1360 (1983) [*Sov. J. Quantum Electron.* **13** 884 (1983)]
174. Balitskas S K, Maldutis É K *Izv. Akad. Nauk SSSR Ser. Fiz.* **49** 1076 (1985) [*Bull. Acad. Sci. USSR Ser. Phys.* **49** (6) 34 (1985)]
175. Zhurkov S N, Eron'ko S B, Chmel' A *Fiz. Tverd. Tela* (*Leningrad*) **24** 733 (1982) [*Sov. Phys. Solid State* **24** 414 (1982)]
176. Kytina I G, Kinber B E *Kvantovaya Elektron.* (*Moscow*) **7** 2427 (1980) [*Sov. J. Quantum Electron.* **10** 1413 (1980)
177. Merkle L D, Koumvakalis N, Bass M *J. Appl. Phys.* **55** 772 (1984)
178. Danileĭko Yu K et al. *Kvantovaya Elektron.* (*Moscow*) **8** 2362 (1981) [*Sov. J. Quantum Electron.* **11** 1445 (1981)]
179. Gomelauri G V et al. *Zh. Eksp. Teor. Fiz.* **79** 2356 (1980) [*Sov. Phys. JETP* **52** 1193 (1980)]
180. Merkulova S P, Shelepin L A, Shubin A A *Tr. Fiz. Inst. Akad. Nauk SSSR* **177** 133 (1987)
181. *Electronics* **60** 91 (1987)
182. Patel C K N, Tam A C *Rev. Mod. Phys.* **53** 517 (1981)
183. Svirezhev Yu M *Nelineinye Volny, Dissipativnye Struktury i Katastrofy v Ékologii* (Nonlinear Waves, Dissipative Structures, and Catastrophes in Ecology) (Moscow: Nauka, 1987)